14 Gas Hydrates in Marine Sediments

Gerhard Bohrmann and Marta E. Torres

14.1 Introduction

Gas hydrates are naturally occurring ice-like crystalline compounds in which gases are trapped within a lattice of water molecules. The presence of gas hydrates is controlled by temperature, pressure and the availability of appropriate gases and water. The first discovery of gas hydrate goes back to 1810, with the pioneering synthesis of chlorine hydrate by Sir Humphrey Davy (Davy 1811). In the 1930s crystalline substances were observed to form spontaneously within natural gas pipelines in permafrost regions, and these deposits, which were clogging the pipelines, were identified as being hydrates of mixed hydrocarbon gases (Hammerschmidt 1934). The recognition that natural gas hydrates can block gas transmission lines, led the hydrocarbon industry to invest in efforts aimed at understanding gas hydrates, and thus begins the modern research in this subject.

Russian scientists (Vasil'ev et al. 1970) were the first to recognize that methane in natural systems could form gas hydrate deposits wherever the pressure and temperature conditions were favourable. These ideas were followed by discovery of gas hydrate, first in the permafrost regions of Russia (Makogon et al. 1971) and Canada's MacKenzie Delta (Bily and Dick 1974), and subsequently in sediments of the Caspian Sea and Black Sea (Yefremova and Zhizhchenko 1974). Interest in these deposits prompted the development of geophysical prospecting tools, which were used to predict the occurrence of gas hydrate in sediments of the Blake Ridge, of the western Atlantic Ocean (Stoll et al. 1971) and elsewhere (Shipley et al. 1979). In the early 1980s, hydrate was recovered from sediments of the Middle America Trench offshore Mexico by the Deep Sea Drilling project (Shipley and Didyk 1982). Since then, deep sea drilling has recovered hydrate from subsurface sediments along the Pacific and Atlantic continental slopes (Kvenvolden 1993). In addition, hydrate has been recovered from many near-surface environments along continental margins worldwide (Mazurenko and Soloviev 2003).

The number of hydrate publications, scientific sessions and workshops dedicated to gas hydrate research has increased substantially during the last 10-15 years, reflecting the development of a broad national and international hydrate research effort in this field. The interest in gas hydrates emerges from the awareness that these deposits may play significant roles in global and regional processes with societal and economic significance. A global hydrate assessment, although still uncertain, suggests that methane hydrates might represent an important future energy resource (Kvenvolden 1998; Collet 2002). In addition, other important hydrate questions that have attracted attention include: 1) Is there a feedback between methane hydrate stability and climate? 2) What is the role of methane hydrate in the carbon cycle? and 3) How much does gas hydrate contribute to seafloor stability on continental slopes?

The purpose of this chapter is to summarize some of the fundamentals of our current understanding of gas hydrate in marine sediments, its interactions with the environment, and recent findings from ongoing research programs that illustrate key aspects of gas hydrate dynamics. We start with general information on the structure and composition of gas hydrates and address their presence and distribution in the marine sediments based on their thermodynamic stability and environmental conditions. Because here we emphasize topics that are relevant to the scope of this textbook, we review the sources and migration mechanism of gases needed to stabilize the hydrate structure; the chemical and isotopic anomalies associated with hydrate formation; and the interaction of hydrates with fluid flow along continental margins.

14.2 Hydrate Crystal Chemistry and Stability of Gas Hydrates

14.2.1 Cages and Three Crystal Structures

Gas hydrates are non-stoichiometric, solid compounds similar to ice crystals (Sloan 1998). In these compounds, also called clathrates (latin clatratus for cage), water molecules form cage-like structures in which low molecular weight gases are enclosed as guest molecules (Fig. 14.1). The gas molecules interact with water molecules through van der Waals (nonpolar) forces. Since no bonding exists between the guest and host molecules, the guest molecules are free to rotate inside the cages, and this rotation can be measured by spectroscopic techniques (e.g. Gutt et al. 1999). Gas hydrate can contain different types of gas molecules in separate cages, depending on the gas composition in the environment of formation. Methane is the main gas in naturally occurring gas hydrates; however H_2S, CO_2 and, less frequently, other hydrocarbons, can also be found within the hydrate structure.

To date gas hydrates have been found to occur in three different crystal structures (Sloan 1998). Structures I and II both crystallize within a cubic system, whereas the third structure (also denominated H) crystallizes within a hexagonal system, analogous to water-ice (Fig. 14.1; Table 14.1). The structure of gas hydrate can be seen as a packing of polyhedral cages. Five types of hydrate cages are known, from which the simplest polyhedron is formed by twelve five-sided polygons (5^{12}) known as pentagonal dodecahedra. This cage is the smallest one that occurs in all three clathrate crystals (Fig. 14.1; Table 14.1). Larger diameter cages can be formed by adding two, four or eight hexagonal faces, and these are denoted as $5^{12}6^2$ in structure I, $5^{12}6^4$ in structure II, and $5^{12}6^8$ in structure H (Table 14.1). In addition, structure H has a medium-sized cavity with square, pentagonal and hexagonal faces ($4^35^66^3$). Figure 1 depicts the five cavities of all three structures that are known to occur naturally.

Structure I is most frequently observed. Its unit cell consists of 8 cages: 2 small (5^{12}) and 6 large cavities ($5^{12}6^2$). Inside each cavity resides a maximum of 1 guest molecule, such that 8 guests molecules are associated with 46 water molecules in structure I ($2[5^{12}]\ 6[5^{12}6^2]\ 46H_2O$). A unit cell of structure II consists of 24 cages, i.e. 16 small cavities (5^{12}) and 8 large ones ($5^{12}6^4$), which account for 136 water molecules ($16[5^{12}]\ 8[5^{12}6^4]\ 136H_2O$). Structure H forms a more complicated crystal composed of 3 small (5^{12}), 2 medium-sized ($4^35^66^3$) and 1 exceptionally large ($5^{12}6^8$) cavity associated with 34 water molecules ($3[5^{12}]\ 2[5^{12}6^4]\ 1[4^35^66^3]\ 34H_2O$).

When all hydrate cages are filled, the three crystal types have similar concentrations of 85 mol% water and 15 mol% guest molecules. Structure I hydrate with CH_4 and C_2H_6 has minimum (stoichiometric) hydration numbers of 5.75 and 7.67, respectively. Only large cavities in the Structure II hydrate are occupied with C_3H_8 (and i-C_4H_{10}), and such hydrates have a hydration number of 17 (e.g. Sloan 1998). However, hydration

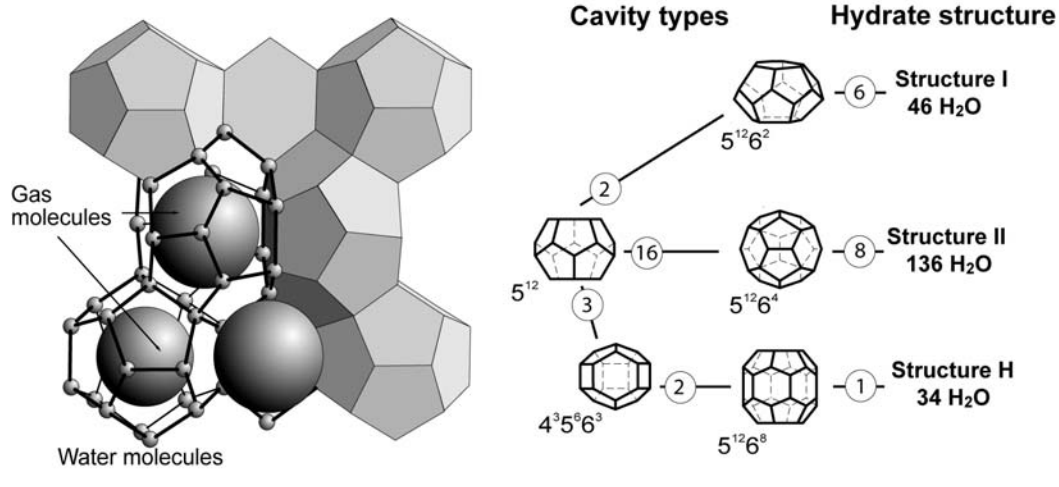

Fig. 14.1 Left: Gas hydrate of type structure I; small spheres are water molecules forming cages; large spheres are gas molecules. Right: Cage types and the number of individual cages forming the three common hydrate crystal structures. The circled numbers denote the numbers of the cages used to form the hydrate structure.

Table 14.1 Summary of some characteristics from the three crystal hydrate structures (from Sloan 1998). * = Estimates of structure H cavities from geometric models.

Hydrate crystal structure	I		II		H		
Symmetry	Cubic		Cubic		Hexagonal		
Cell constant (Å)	12.03		17.31		a = 12.26; c = 10.17		
Cavity	Small	Large	Small	Large	Small	Medium	Large
Description of cavity	5^{12}	$5^{12}6^2$	5^{12}	$5^{12}6^4$	5^{12}	$4^35^66^3$	$5^{12}6^8$
Number of cavity / cell unit	2	6	16	8	3	2	1
ø cavity radius (Å)	3.8	4.33	3.91	4.73	3.9*	4.06*	5.71*
Coordination number	20	24	20	28	20	20	36
n H_2O/unit cell	46		136		34		

numbers of naturally occurring gas hydrates are highly variable, and are generally depleted in gas relative to its stoichiometric value. Samples from the Middle America trench off Guatemala and from the Green Canyon area of the northern Gulf of Mexico have hydration numbers of 5.91 and 8.2, respectively (Handa 1990). Matsumoto et al. (2000) reports a hydration number of 6.2 for hydrate from the Blake Ridge.

14.2.2 Guest Molecules

Gas molecules in sufficient amount are a prerequisite to stabilize the hydrate structures. In principle, the occupied hydrate cage is a function of the size ratio of the guest molecule to the host cavity. Figure 14.1 illustrates the guest/cavity size ratio for hydrates formed of a single guest component in either structure I or structure II (Sloan 1998). Molecules smaller than 3.5 Å will not stabilize hydrates and those larger than 7.5 Å are too large to fit in the cavities of structures I and II. Some molecules are too large to fit the smallest cage of each structure (e.g. C_2H_6 fits in $5^{12}6^2$ of structure I), whereas other molecules such as CH_4 and N_2 are small enough to enter both cavities (denoted as either 5^{12} and $5^{12}6^4$ in structure I). At pressures greater than 0.5 kbar two N_2 molecules can be accommodated in the $5^{12}6^4$ cage (Kuhs et al. 1996). The largest molecules determine which structure will form. Because propane and i-butane are present in many thermogenic natural gases, they will cause structure II to form. In such cases methane will occur in both cages of structure II and ethane will enter only the $5^{12}6^4$ cage of structure II.

Table 14.2 shows the size ratio of several gas molecules within each of the four cavities of structures I and II. A ratio of molecule to cage size of approximately 0.9 is necessary for stability of a hydrate composed of a single gas. When the size ratio exceeds unity, the gas will not fit within the cage structure and hydrate will not form. When the ratio is significantly less than 0.9 the molecule cannot lend significant stability to the cage (Sloan 1998).

Structure I, which is by far the most commonly found in marine deposits, contains small guest molecules with diameters ranging from 4 to 5.5 Å.

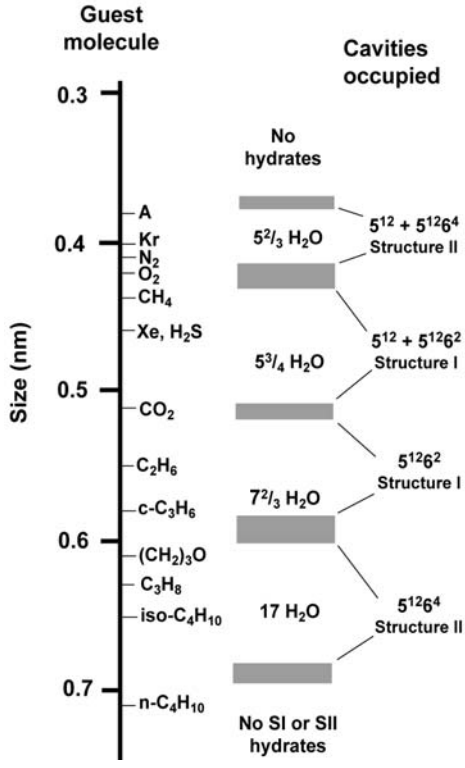

Fig. 14.2 Guest molecules versus hydrate cage size range (from Sloan 1998). Left line shows the size of typical hydrate-forming guest molecules. The number of water molecules in gas hydrates shown, corresponds to single guest gas occupants listed on the left. The related type of structures formed are listed on the left. As an example, methane has a typical hydration number of $5^3/_4$ and occupies both cages of structure I.

Table 14.2 Ratios of molecular diameters (obtained from von Stackelberg and Müller 1954) to hydrate cavity diameters for various gases, including those commonly found in natural gas hydrate (from Sloan 1998). ^{F} = indicates the cavity occupied by a single guest.

Molecule	Guest diameter Å	Structure I		Structure II	
		5^{12}	$5^{12}6^4$	5^{12}	$5^{12}6^4$
N_2	4.10	0.804	0.700	0.817 ^{F}	0.616 ^{F}
CH_4	4.36	0.855 ^{F}	0.744 ^{F}	0.868	0.652
H_2S	4.58	0.898	0.782	0.912	0.687
CO_2	5.12	1.00	0.834	1.02	0.769
C_2H_6	5.50	1.08	0.939 ^{F}	1.10	0.826
C_3H_8	6.28	1.23	1.07	1.25	0.943 ^{F}
i-C_4H_{10}	6.50	1.27	1.11	1.29	0.976 ^{F}
n-C_4H_{10}	7.10	1.39	1.21	1.41	1.07

Structure I cages can therefore enclose gas molecules that occur naturally in marine sediments and are smaller in diameter than propane, such as CH_4, CO_2 or H_2S. The natural occurrence of this crystal structure depends on the presence of biogenic gas in sufficient amounts, as commonly found in sediments of the ocean floor underlying areas of high biologic productivity. Cubic structure II generally occurs with guest molecules ranging between 6-7 Å. Hence, it contains natural mixtures of gases with molecules bigger than ethane and smaller than pentane, and it is therefore usually confined to areas where a thermogenic gas is present in the sediment. Hexagonal structure H may be present in either environment, but only with mixtures of both small and very large (8-9 Å) molecules, such as methylcyclohexane.

The smallest guest molecules that form hydrate structure II have diameters smaller than 4 Å, (e.g. Ar, Kr, O_2 and N_2). Such nitrogen and oxygen clathrates are known as air clathrates, and have been observed in ice-cores from Antarctica and Greenland below ~ 1100 m. In these samples, individual air bubbles have reacted with polar ice under high pressure to form clathrates (Shoji and Langway 1982).

14.2.3 Stability and Phase Boundaries of Gas Hydrates

The presence of gas hydrates is controlled by several factors, among which, temperature, pressure, ionic strength of the water and gas composition and abundance are key parameters (Sloan 1998). The pressure/temperature conditions required for pure methane hydrate stability are illustrated in Fig. 14.3. In this case, methane hydrate is stable at temperatures higher than 15°C only at high pressures (> 10 MPa). At lower pressures, the stability of methane hydrate requires colder temperatures (e.g. for P < 6 MPa; T< 10°C). In the pressure/temperature field, the phase boundary is determined by the gas composition and also by the ionic strength of the water. The presence of CO_2, H_2S, ethane and/or propane will have the effect of shifting the stability curve to a higher temperature at a given pressure, increasing the stability of methane hydrate. The presence of dissolved ions in the pore fluids, on the other hand, inhibits the stability of hydrate. There is a –1.1°C offset in dissociation temperature of methane hydrate in 33% NaCl, relative to that of hydrate formation in pure water (e.g. Dickens and Quinby-Hunt 1994). Thus, an increase in salinity of the fluids from which the hydrate is forming shifts the phase boundary to the left (Fig. 14.3).

Accurate and precise prediction of the P/T conditions for natural gas hydrate stability is a field of active research, and numerous methods for predicting methane hydrate stability can be found in the literature (summarized in Sloan 1998). Dickens and Quinby-Hunt (1994) estimate the P/T conditions for hydrate stability by interpolating experimentally determined dissociation data. Since their experiments were conducted in both seawater and freshwater matrices, their results are useful in evaluating the effects of pore fluid salinity. Other methods to estimate the stability conditions are based on minimizing the Gibbs Free Energy of the system. The most commonly used of these computer-based methods is the Sloan (1998) PC-DOS program CSMHYD, which allows for stability estimates at varying salinities. Simpler calculation methods are also available for the rapid estimation of hydrate formation conditions (Carroll 2003).

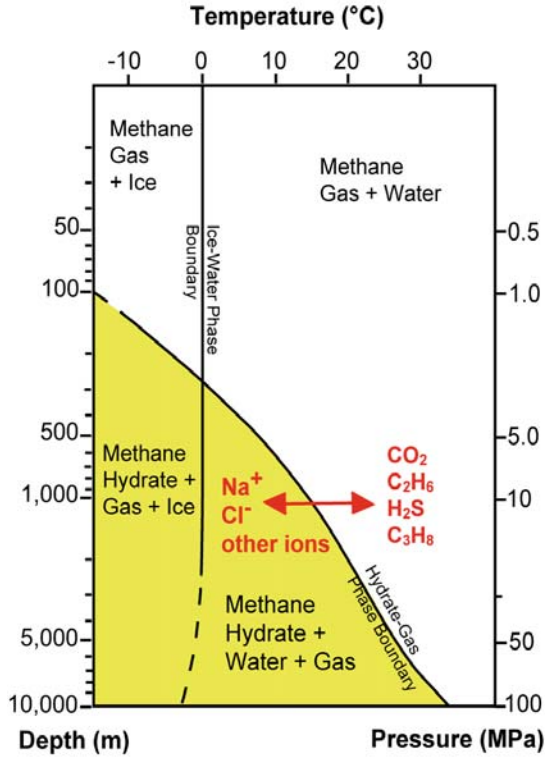

Fig. 14.3 Phase diagram showing the boundary between methane hydrate (in yellow) and free methane gas (white) for a pure methane/H_2O system. Addition of ions shifts the boundary to the left, decreasing the P/T stability field. The presence of gases like carbon dioxide, hydrogen sulphide or other high-molecular hydrocarbons shifts the curve to the right, thus increasing the P/T field in which methane hydrate is stable (after Kvenvolden 1998).

14.3 Hydrate Occurrence in the Oceanic Environment

14.3.1 Gas Hydrate Stability Zone in Marine Sediments

Gas hydrates form wherever appropriate physical conditions exist and concentrations of low molecular weight gases, mostly methane, exceed saturation. The P/T factors for the presence of methane hydrates (Fig. 14.3) are present in marine sediments as shown by the phase boundary in Fig. 14.4. The dashed line shows a typical temperature profile through the water column in the Atlantic Ocean. Near surface temperatures are too warm and pressures too low for methane hydrate to be stable. Below the major thermocline there is change in the temperature gradient, and the temperature profile intersects the phase boundary at ~450 m water depth, which defines the upper limit for methane hydrate stability in that part of the ocean. If methane is sufficiently abundant, methane hydrate would form. However, since the density of hydrate is around 0.913 g cm^{-3} (Sloan 1998) any crystalline hydrate that may form in the water column (e.g. at sites of methane discharge) will rise due to its relative buoyancy and it will dissociate when it reaches depths above its stability field. However, if methane hydrate forms within the sediment pore space, it will be bound in place. If water temperatures are colder the upper limit for methane hydrate is shallower. This limit of

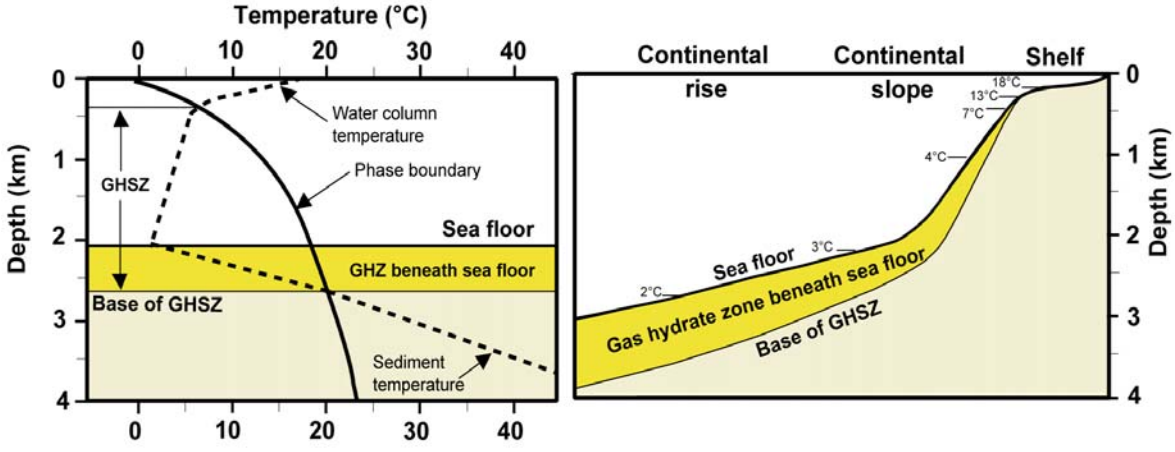

Fig. 14.4 Left: Stability field of pure methane hydrate at normal seawater salinity, as defined by temperature and pressure expressed as water depth. Intersections of the temperature profiles (stippled lines) with the phase boundary (heavy line) define the area of the gas hydrate stability zone (GHSZ). Right: Inferred thickness of the gas hydrate zone in sediments at a schematic continental margin assuming a typical geothermal gradient of 28°C km^{-1}. Typical bottom water temperatures are marked, and range from 18°C on shallow shelf regions to 2°C at the bottom of the continental rise (after Kvenvolden and McMenamin 1980).

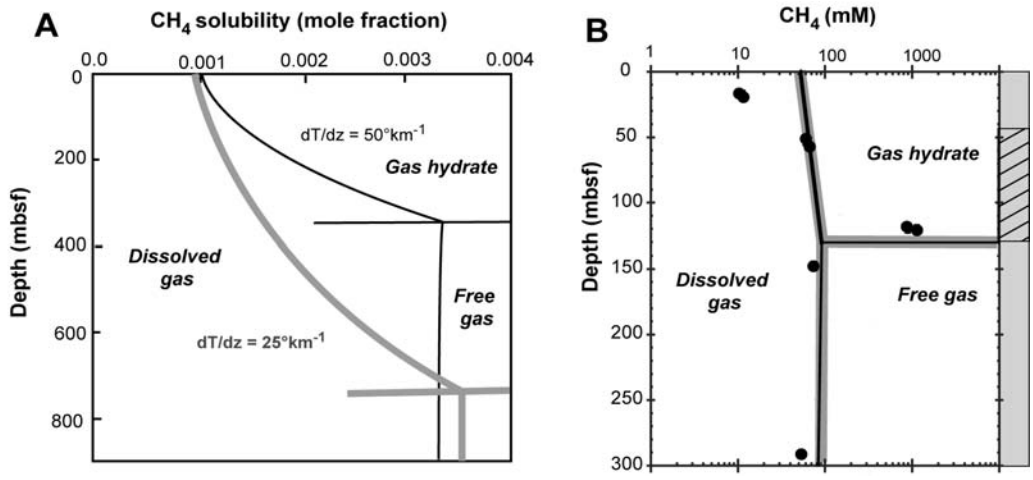

Fig. 14.5 A. Methane solubility as a function of depth in the sediment (mbsf = meters below seafloor) based on thermodynamic functions and assuming two different geothermal gradients of 50° km^{-1} (black line) and 25° km^{-1} (gray line). It illustrates the effect of temperature changes on the vertical gradient of methane solubility and on the depth of the GHSZ, which is defined by the discontinuity in the slope of the gas solubility curves and demarked by horizontal lines. In this example the pressure is assumed to be hydrostatic. The water depth is assumed to be 2000 m, and bottom water temperature used is 2.5° C (from Zatsepina and Buffet 1997). **B.** Approximate phase boundaries where dissolved gas, gas hydrate and free gas are predicted for Site 1245, drilled on 880 meters of water depth during ODP Leg 204 offshore Oregon. Uncertainties (~30%) in the position of these boundaries result from variations in subsurface thermal gradient, gas composition and pore fluid salinity. The closed circles represent methane concentration in sediments recovered at in situ pressure, revealing that there is not enough methane in the upper 45 meters to support hydrate formation, thus defining the gas hydrate occurring zone (GHOZ) as the interval between 45 and 135 mbsf. These inferences are consistent with observations of hydrate in the sediment, as indicated by the shaded region in the column to the right (from Tréhu et al. 2003).

hydrate occurrence in sediments is deeper in closed ocean basins where the temperature of the bottom water is higher. For example, within the Black Sea where the bottom water temperature is 9°C, the upper limit of hydrate stability is around 700 m water depth (Bohrmann et al. 2003). In contrast, in the polar oceans, gas hydrate can be stable in 300 m of water (Kvenvolden 1998).

The local geothermal gradient in marine settings determines the temperature profile below the sea-floor (Fig. 14.4 dashed line in the sediment sequence). As temperature in the sediments increases with depth, the sediment temperature will eventually get high enough to cross the phase boundary, such that gas hydrate will no longer be stable beneath this depth. Other factors like the gas composition and salt content of the pore water influence the precise location of the lower boundary of the gas hydrate stability zone (GHSZ). Thus, the base of the GHSZ is itself a phase boundary. Since the geothermal gradient is often quite uniform across broad regions beneath the seafloor, the thickness of the GHSZ is quite constant for a given water depth. However, a change in water depth will influence the thickness of the hydrate stability zone (Fig. 14.4). Due to the P/T conditions for hydrate stability, the thickness of the GHSZ can reach 800 to 1000 m below seafloor in deep water areas, and the base of the GHSZ will shoal up as water depth decreases (Fig. 14.4).

Even though P/T conditions in most of the ocean floor lie within the hydrate stability field, no such deposits are found in the abyssal plain because there is not enough gas in these sediments to stabilize the hydrate structure. This fact illustrates the third fundamental requirement for gas hydrate formation. In addition to moderately high pressures and low temperatures, gas hydrates will only form if the mass fraction of methane exceeds its solubility. Methane solubility itself is a function of pressure and temperature. At depths within the GHSZ, the equilibrium concentration in the presence of hydrate decreases almost exponentially towards the seafloor (Fig. 14.5A). At greater depths, the equilibrium is defined between aqueous solution and free gas. In Figure 14.5B this relationship is shown for sediments recovered from the flanks of Hydrate Ridge (ODP Site 1245), in the Cascadia margin. Here the entire sediment column above 134 meters lies within the GHSZ; however, sediments above 40 meters do not have enough methane to support hydrate formation (Tréhu et al.

2003). Consistent with inferences based on methane concentration measured on cores collected at in situ pressures, gas hydrate in these sediments is only present between 45 and 134 meters, in what is known as the gas hydrate occurrence zone (GHOZ).

14.3.2 Seismic Evidence for Gas Hydrates

The first indications of methane hydrate in marine sediments were based on the observation of a seismic reflection called "bottom-simulating- reflector" or BSR, because it approximately mimics the sea-floor (Shipley et al. 1979). The BSR cuts across reflections of stratigraphic origin, making it readily apparent in marine seismic records (Fig. 14.6). This reflection occurs approximately at the depth where the base of the gas hydrate stability zone is predicted based on thermodynamic equilibria (e.g. Tucholke et al. 1977; Shipley et al. 1979; Hyndman and Spence 1992). Because of the temperature dependence of hydrate stability, the depth of the BSR provides a means of mapping the thermal gradient and heat flux in the overlying sediment (e.g. Davis et al. 1990). The negative polarity of this reflection indicates that it results from a decrease in acoustic impedance (defined as a product of density and seismic velocities) with depth. Fig. 14.6 illustrates the presence of a BSR on Blake Ridge, which demarks the impedance contrast between gas hydrate-cemented sediments above the BSR and the sequence below it, where free gas is present.

Although some details of the seismic reflection properties are not yet fully understood, it appears that the strength and the characteristics of the BSR is determined by the presence of free gas below the gas hydrate zone (Paull et al. 1996). The presence of free gas represents a very large change in seismic velocity, and therefore produces a very strong and sharply defined reflection. Theoretical models (Xu and Ruppel 1999) and synthetic studies (Wood and Ruppel 2000) indicate that the BSR is not a necessary condition for the presence of hydrate, as it only occurs when there is free gas beneath the distinct gas hydrate phase boundary. If there is no free gas below a deposit of gas hydrate, there will be no BSR. Indeed, sediments containing gas hydrate have been recovered from areas where there is no BSR (Mathews and von Huene 1985).

Models on gas hydrate concentration based on analyses of the BSR properties depend on a number of poorly constrained parameters, and thus these geophysical estimates need to be calibrated against direct measurement of hydrate abundance. The *Ocean Drilling Program* has sampled various BSR horizons on the continental slopes around the Pacific Rim (e.g. Peru, Chile, Costa Rica, Oregon/Washington, Japan) and on the passive US Atlantic margin (Blake Ridge) with the aim of understanding gas hydrate characteristics, distribution and concentration in continental margin settings. These efforts, in particular recovery of samples under in situ pressure and calibration of

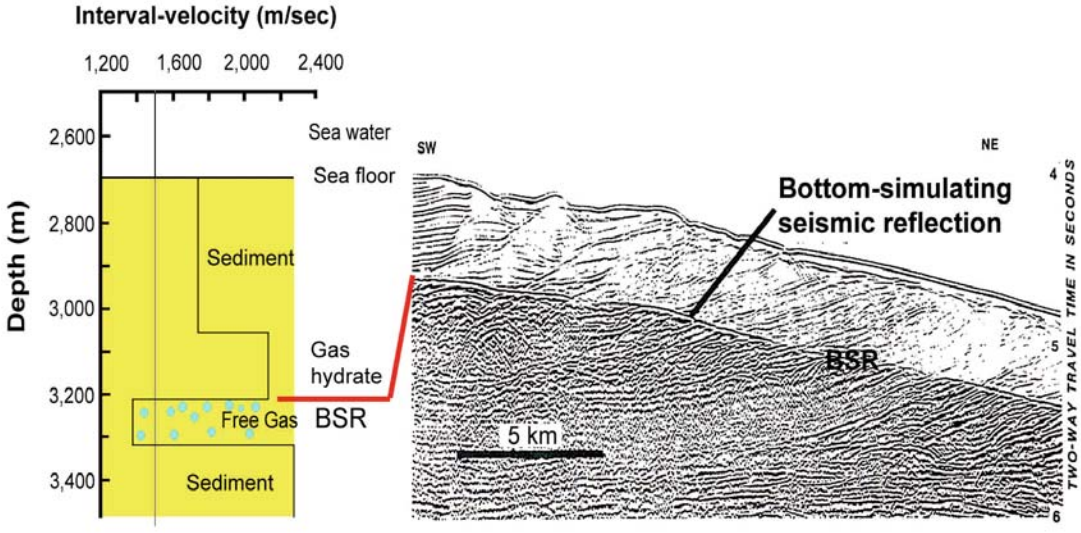

Fig. 14.6 Seismic record from Blake Ridge (Shipley et al. 1979), showing a distinct reflection, known as bottom simulating reflection (BSR), which indicates the presence of methane hydrate within sediments (right). Below the BSR there are strong reflections caused by free gas in the pores. A seismic velocity model (left) shows the strong contrast of velocity across the BSR.

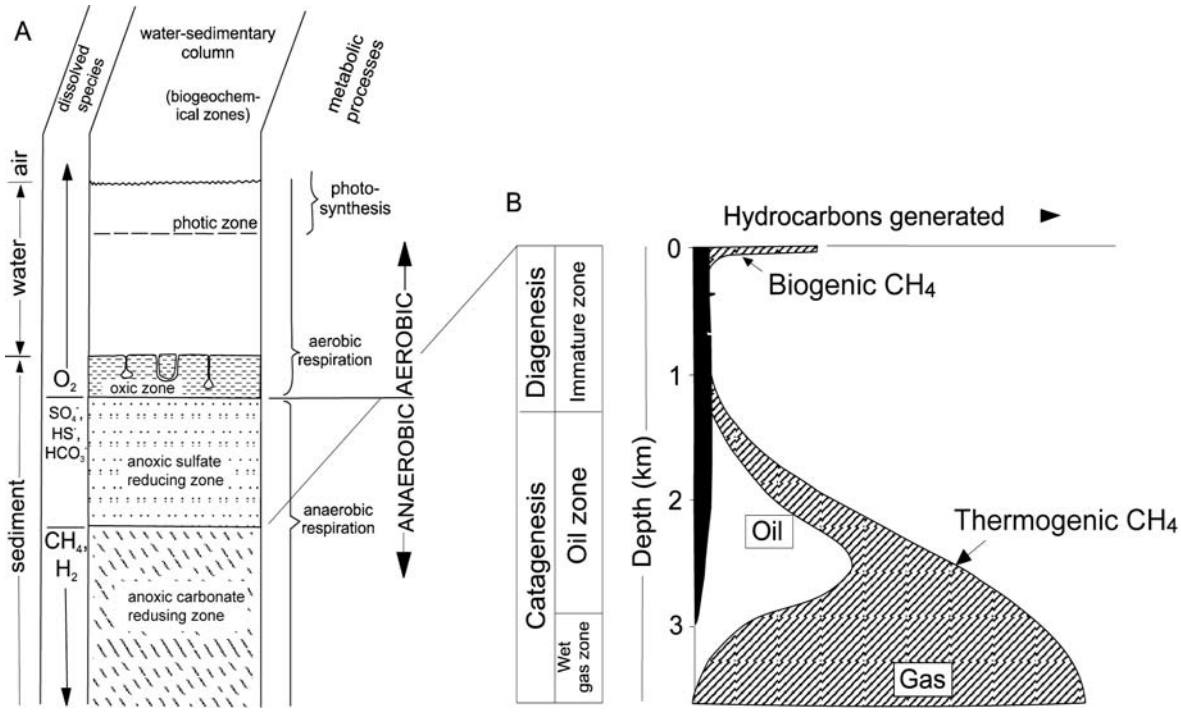

Fig. 14.7 **A:** An idealized cross section of a marine organic rich sedimentary environment, showing biogeochemical zones in ecological succession (from Claypool and Kaplan 1974). **B:** Hydrocarbon generation by diagenesis and catagenesis processes as a function of depth (from Tissot and Welte 1992).

various proxies for hydrate abundance (e.g. Tréhu et al. 2004a) will continuously improve our imperfect knowledge of the distribution of gas hydrate in the seafloor.

14.3.3 Generation of Gases for Hydrate Formation

In their classic work on the origin and distribution of methane in marine sediments, Claypool and Kaplan (1974) place biogenic methane generation within the ecological succession of microbial ecosystems in the marine sedimentary environment (Fig. 14.7A). These zones are characterized by successively less efficient modes of respiratory metabolism, which are interlinked by microbially-induced environmental changes: onemicrobe's metabolic waste serves as substrate for another organism. Details of the microbiological pathways during early organic matter diagenesis are covered in chapter 4. Here we focus on the generation of methane needed for gas hydrate formation.

Biogenic methane is produced as an end product of the metabolism of a diverse group of obligate anaerobic archaea (killed by even traces of oxygen), generally known as methanogens. These organisms can live in a wide range of temperature, salinity and pH, but are limited in the substrates they can utilize for growth. The most important substrates for bacterial methanogenesis are acetate (acetoclastic methanogenesis) and $H_2 : CO_2$ (carbonate reduction). A detailed description of the pathways involved in methanogenesis from the bacterial decay of organic matter in marine and freshwater sediments is given by Wellsbury et al. (2000).

Deep ocean sites containing gas hydrate have been analyzed to determine bacterial numbers, activity rates, cultural metabolic groups and estimates of biodiversity using molecular genetic analyses (Reed et al. 2002; Colwell et al. 2004). Bacterial population usually decreases in number with increasing depth (Wellsbury et al. 2000), but significant bacterial counts and activities have been measured within and beneath the GHSZ in Blake Ridge and Hydrate Ridge sediments (Wellsbury et al. 2000; Colwell et al. 2004).

Deeper in the sediment, thermal alteration of organic matter generates methane and higher order

hydrocarbons by catagenesis (Fig. 14.7B). Catagenesis occurs within the temperature range of 50° to 200° C, and gases (methane to butane) are produced at rates that are proportional to temperature.

At typical oceanic geothermal gradients of 20° to 50° C km^{-1}, sediment depths larger than 1km are required to produce significant amounts of gas by thermochemical action. Because thermogenic gas generation occurs at temperatures significantly deeper than those found within the GHSZ, high concentration of thermogenic gases within the GHSZ generally indicates the existence of a hydrocarbon migration pathway.

Biogenic and thermogenic gases can usually be distinguished on the basis of chemical and isotopic composition. Biological gas is dominantly composed of methane, which is depleted in ^{13}C relative to thermogenic methane (Whiticar 1999), as shown in Figure 14.8A. Methane derived from $H_2 : CO_2$ is in general more depleted than that derived from acetate. The hydrogen isotope signature may also provide information on the metabolic pathways, as acetate fermentation yields methane with a δD value lower than –250 ‰, whereas carbonate fermentation leads to δD values ranging from –150 to –250 ‰ (Whiticar et al. 1986).

Isotopic discrimination, nevertheless, should be used with caution. Various environmental factors such as substrate limitation and temperature may obscure the $\delta^{13}C$ distinction between thermogenic and biogenic sources. In addition, laboratory experiments have shown that during acetate methanogenesis some of the methyl hydrogen atoms can exchange with water, affecting the δD of the methane produced (de Graaf et al. 1996).

The ratio of methane (C_1) to heavier hydrocarbons, usually expressed as the sum of ethane and propane ($C_2 + C_3$), also provides information on the methane source. Biogenic gas consists predominantly of methane and typically has values for the $[C_1/ (C_2 + C_3)]$ ratio that are greater than 10^3. In thermogenic gas, this ratio is usually less than 100 (Bernard et al. 1976). Although recent studies indicate that bacterial activity can indeed generate higher level hydro-carbons (C_2 to C_4), they do not occur at high enough concentration. In Figure 5B, the hydro-carbon ratio is plotted against the methane isotopic composition, showing the thermogenic versus biogenic gas fields.

Elemental and isotopic analyses of hydrate samples from a variety of settings show that microbial activity is the dominant methanogenic pathway in marine sedimentary environments, such as Blake Ridge (Dickens et al. 1997), Hydrate Ridge (Suess et al. 2001), Nankai Trough (Takahasi et al. 2001), Congo-Angola basin (Charlou et al. 2004) and the Sea of Okhotsk (Ginsburg et al. 1993). Hydrates with thermogenic methane have been recovered from the Gulf of Mexico (Brooks et al. 1984) and the Caspian Sea (Ginsburg et al. 1992).

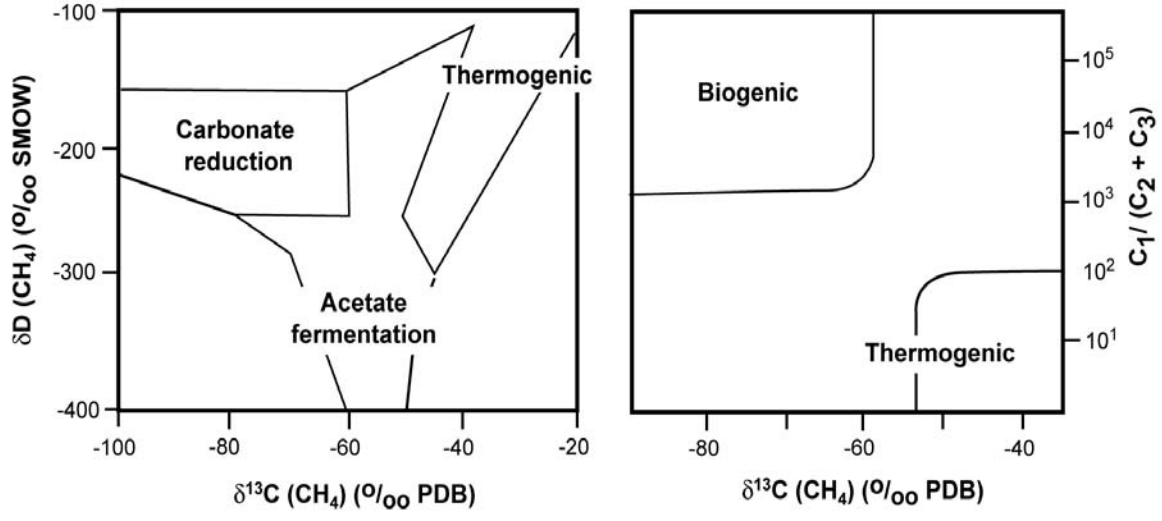

Fig. 14.8 Discrimination of biogenic and thermogenic methane sources based on **A**. The carbon and hydrogen isotopic composition of the methane (after Schoell 1988), and **B**. The ratio of methane (C_1) to higher hydrocarbons ($C_2 + C_3$) plotted against the carbon isotopic composition of methane (from Claypool and Kvenvolden 1983).

14.3.4 Methane Transport and Hydrate Formation

If methane, either from biogenic or thermogenic sources, is present in high enough concentration to stabilize the hydrate structure at thermodynamically favourable conditions (Figs. 14.3 and 14.4), it will combine with water to form hydrate. For methane hydrate to occur, the rain rate of carbon to the seafloor must be high enough to supply the required methane via degradation of organic matter in the sediment. Hydrate stability requires gas concentration in the hydrate at least two orders of magnitude greater than gas solubility in the liquid phase. Thus, methane generation and transport processes are key factors for constraining global hydrate inventories.

Hydrate Formation by in situ Biogenic Methane Generation and Transport in Advecting Fluids

The amount of biogenic methane is essentially controlled by both the availability and reactivity of organic matter in the upper hundreds of meters of the sedimentary sequence. Davie and Buffett (2001, 2003) demonstrated the critical need for quantitative models of biogenic methane production to describe the distribution of gas hydrate in the top few hundred meters of sediment. Key parameters are rates of sedimentation, quality and quantity of the organic matter and biological activity rates. They show that hydrate accumulation from in situ production in sediment with a TOC of 1.5%, will be less than 7% of the pore volume

If in situ production of biogenic methane is not adequate to support observed accumulations within the GHSZ, then additional methane must migrate from below. Paull et al. (1994), proposed a mechanism to concentrate methane via recycling at the base of the GHSZ in the Blake Ridge hydrate-bearing province. Progressive burial and subsidence through geologic time shifts the base of the GHSZ upward, so that deep-seated hydrate decomposes. As hydrate dissociates, the methane solubility is surpassed, and free gas permeates fissures in the overlying hydrate stability layer, enhancing gas hydrate contents via precipitation of the “recycled” methane.

Davie and Buffett (2001) also show that both in situ methane production and transport in upward migrating saturated fluids are needed to explain the dissolved chloride profiles observed in Blake Ridge sediment. Similarly, Hensen and Wallmann (2005) show that, although organic carbon degradation in the upper sediments of the Costa Rica margin can account for 0.4 to 1.1 % of hydrate content of the sediment, it alone cannot explain the hydrate distribution in this region. Furthermore they show that fluid flow may increase the total amount of hydrate that can be formed from the organic reservoir in this margin by more than 50%.

Fluid flow can scavenge methane from a broad region, thus it is expected that active margins with pervasive fluid transport would have higher abundance of gas hydrate. Nevertheless, even the small rates of fluid flow in passive margins, play a controlling role on the accumulation of gas hydrate (Egeberg and Dickens 1999). In fact, using a mechanistic model for the distribution of hydrate in marine sediment, Buffet and Archer (2004) conclude that the global inventory of gas hydrate is particularly sensitive to both, methane generation from organic matter and the rate of fluid flow.

Methane Transport in the Gas Phase

Most disseminated hydrate in marine sediment is thought to occupy less than 8% of the pore space of sediments integrated over the GHSZ. However, there are regions where massive hydrate is known to form near or at the seafloor. These shallow hydrate deposits are usually associated with areas of fluid venting and gas ebullition (Mazurenko and Soloviev 2003). Geochemical modelling of the shallow hydrate at the summit of southern Hydrate Ridge demonstrates the need for methane transport in the gas phase. Because of the low solubility of methane in water, advection of methane-saturated water is not enough to sustain the rapid hydrate growth in this system (Torres et al. 2004). In general, methane hydrate will only form large concentrated deposits where gas flow is present.

Methane concentration increases with depth in the sediment due to a combination of processes including microbial generation, methane recycling at the base of the GHSZ, and thermochemical generation at depth. When methane concentration in the pore water exceeds saturation, methane gas will exolve. However, the difficulty of nucleating bubbles of small size in fine-grained porous media can lead to significant supersaturations. Clennell et al. (2000) provide a

comprehensive review of processes involved in movement of methane in marine sediment, with an emphasis on how porosity, pore size distribution and permeability of the sediment control the rates and mode of transport of gas. They discuss issues associated with capillary theory, multi-phase flow, invasion percolation, catenary transport, and flow in faults and fractures, which are important to fully understand gas hydrate formation dynamics in marine systems, but are beyond the scope of this book. Here we provide a simplified overview of two mechanisms that are important in gas transport, but refer the reader to Clennell et al. (2000) for a more quantitative treatment of these processes.

Gas Migration Induced by Diapirism

In regions of known diapirism, when overpressure builds up due to gravitational or fluid loading, gas migration can occur via faults and fractures. Here a combination of overpressure and the buoyancy of expanding gas drive the flow. If the flow reaches the surface, a mud volcano will form. The high advective rates transport methane bearing fluids, and relatively high temperatures and sometimes enhanced salinities preclude gas hydrate formation during methane migration to the seafloor. These characteristics are typical in regions such as the Gulf of Mexico (Ruppel et al. 2005), where overpressured fracture zones that surround moving salt diapirs provide active conduits for vertical migration from deep reservoirs to shallow subsurface (e.g. Sassen et al. 1994). Carbon elemental and isotopic analyses demonstrate high input of thermogenic methane in this region (Sassen et al. 1994). Other examples exist in the Eastern Mediterranean (De Lange and Brumsack 1998) and the Black Sea (Bohrmann et al. 2003). Another region of shallow hydrate formation associated with mud volcanism is the Håkon Mosby mud volcano in the Norwegian-Greenland Sea. Mud flow in the volcano is thought to be driven by the rise of lower density pre-glacial biogenic silica oozes buried beneath higher density glacial marine sediments. The methane in the hydrate here has a mixture of thermogenic and biogenic sources (Lein et al. 1999). A temperature model (Fig. 14.9) has been used to show how these fast-rising hot fluids serve as a methane transport mechanism to the seafloor, where hydrate content ranges from 10-20% to 0% by weight (Ginsburg et al. 1999).

Because fluid migration in diapir systems bring large amounts of gas to very shallow sub-bottom depths, gas hydrate formation in these soft sediments can create its own space by deforming the surrounding matrix (Bohrmann et al. 1998, Clennell et al. 1999; Torres et al. 2004). Thus, gas hydrate associated with rapid transport along faults and fractures are generally more localized and massive than biogenic deposits commonly found dispersed within the sediment.

Gas Pressure Driven Flow

Another driving force for methane transport is the generation of critical pressures in the gas phase (Flemings et al. 2003; Tréhu et al. 2004). Interconnection of gas-filled pores below the GHSZ transmits hydrostatic pressures from greater depths because of the low density of the gas phase. The excess (non-hydrostatic) pressure at the top of the gas layer may be sufficient to

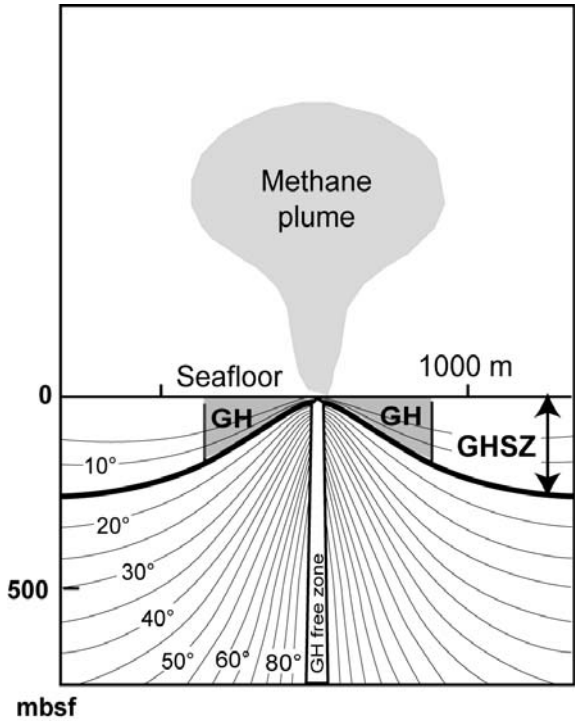

Fig. 14.9 Distribution of gas hydrate (after Egorov et al. 1999) superimposed on a schematic vertical model of the temperature field (after Ginsburg et al. 1999) in the Håkon Mosby Mud Volcano. The gas hydrate stability zone (GHSZ, shown by bold lines) is determined by pressure and temperature conditions; the zone of gas hydrate (GH) accumulation depends on both the thermal gradient and the flux rate of methane.

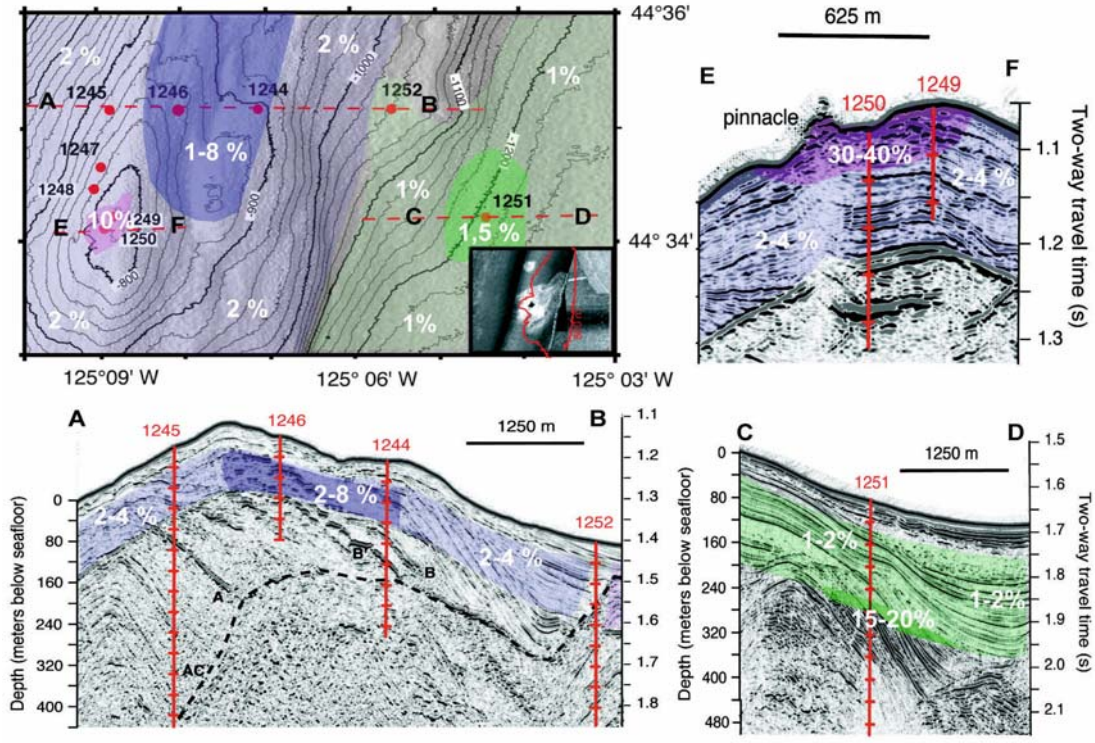

Fig. 14.10 Average gas hydrate concentrations in sediments from southern Hydrate Ridge deduced by drilling during ODP Leg 204 using a multi proxy approach (from Tréhu et al. 2004a). Upper left: Bathymetric map of the region studied during ODP Leg 204 and the lateral extend of zones of different gas hydrate content, estimated by averaging the data from the sea floor to the BSR. Location of seismic profiles and the drill sites are also shown. Gas hydrate concentrations as percentage of pore space shown in white bold numbers were estimated as average concentrations in the GHSZ.

fracture the sediments and drive gas towards the seafloor. This process has been postulated for both passive (Flemings et al. 2003) and active (Tréhu et al. 2004b) regions, where the volume fraction of gas is ≥ 10% (Flemings et al. 2003).

In their analyses of past and future state of the hydrate reservoir, Buffett and Archer (2004b), suggest that if elevated gas pressures do occur as a transient response to warming, a rapid release of methane may be triggered by the development of critical pressures in the gas phase. Critical gas pressure below the base of the gas hydrate stability zone can trigger vertical migration of free gas to the seafloor.

14.3.5 Gas Hydrate Accumulation in Sediments and Fabric of Natural Gas Hydrates

Drilling of marine sediment cores as well as seafloor sampling by research vessels confirmed the presence of gas hydrate in sediments defined by the stability field as described in section 14.3.1. Conventional research vessels are only able to sample shallow sediments close to the seafloor, thus drilling campaigns are needed to investigate the distribution of gas hydrates deeper within the stability field. Because gas hydrates decompose rapidly when removed from the high-pressure, deep-water environments in which they form, the in situ distribution of gas hydrate must be estimated using various proxy techniques, each of which may have different sensitivity and spatial resolution (Tréhu et al. 2004a). Leg 164 of the Ocean Drilling Program (ODP) drilled several sites on the Blake Ridge, in the first dedicated academic effort to investigate naturally occurring gas hydrates in marine sediments (Paull et al. 1996). Estimates made using diverse gas-hydrate proxies revealed that gas hydrate occupies ~ 1% to 10% of the pore space in the sediment interval from 200 to ~450 mbsf. The hydrate occurs dispersed within the pore-space of fine-grained sediments or within fractures and faults (Paull et al. 1996). The distribution of fine grained gas hydrate within the lithologically uniform drift sediments of the

Blake Ridge was surprisingly heterogeneous and could not be explained in detail, except for the observation of two weakly defined zones where higher hydrate concentrations may indeed be caused by small differences in lithology.

Researchers involved in ODP Leg 204 generated the first high-resolution data set on the three-dimensional distribution of gas hydrate within Hydrate Ridge, in the Cascadia subduction zone (Tréhu et al. 2003). Several gas hydrate proxies were combined, and thus, the problem of spatial under-sampling inherent in methods traditionally used for estimating the gas hydrate was overcome (Tréhu et al. 2004a). The average gas hydrate content of sediments within the gas hydrate stability zone was estimated to be 1-2% of the pore space. Patchy zones of locally higher concentrations on the ridge flanks occur below ~ 40 mbsf, are structurally and stratigraphically controlled and occupy up to 20% of the pore space (Fig. 14.10). In contrast to this overall hydrate distribution, a high average gas hydrate content of 30-40% of pore space was found on the upper 30-40 mbsf at the ridge summit. Cores containing hydrate in massive chunks, lenses, plates and nodules, where recovered from an area where there is persistent and vigorous venting of methane gas (Heeschen et al. 2003).

A variety of gas hydrate samples were recovered from the southern summit of Hydrate Ridge by deploying a TV-guided grab on visible hydrate outcrops (Suess et al. 1999, 2001). Due to a self-preservation effect (Yakushev and Istomin 1992), massive hydrate shows little indication of decomposition, and samples from the inner part of the TV-grab appeared to be relatively pristine (Fig. 14.11). Scanning electron microscopic work revealed that only in very porous samples there was water-ice formation (Fig. 14.11B; Kuhs et al. 2004). On a macroscopic scale, pure white gas hydrate occurs in layers or joints several millimeters to centimeters thick. The layers are generally oriented parallel to the bedding planes and in some cases very massive hydrates of up to 10 cm in thickness have been observed (Fig. 14.11). Gas hydrate either fills large pore space in fractures or joints, or it creates its own space by fracturing or pushing apart the sediment framework during growth, most often along bedding planes. The result of such an active crystal growth is that the original sediment fabric is disturbed and mud clasts are formed. In many cases internal brecciation of the sediment was observed in which the angular edges of the clasts often fit with the edges of neighboring clasts (Fig. 14.11A).

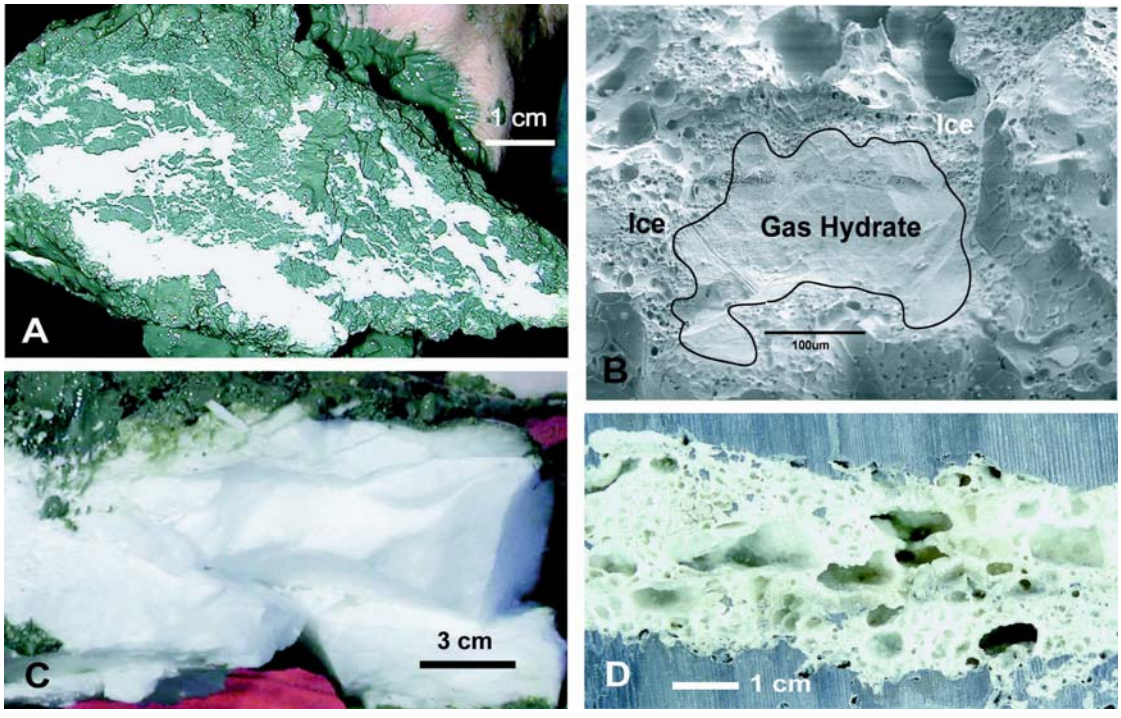

Fig. 14.11 Hydrate fabrics typical for shallow gas hydrate specimens (A, C and D): sediment-hydrate interlayering (A), pure dense hydrate layer (C), and highly porous bubble-shaped framework (D) B: Field-electron scanning micrograph of hydrate surrounded by bubble-shaped ice.

The internal fabric of pure gas hydrate has a peculiar structure with pores that result from rising methane gas. Such pores occur in variable sizes, and in some specimens very large pores of up to 3-4 cm in diameter can be observed (Fig.14.11D). The fabric is similar to that of gas hydrates experimentally formed on the sea-floor (Brewer et al. 1997). There are several lines of evidence that support migration of methane gas from a reservoir located beneath the GHSZ, which either turns into macroscopic porous gas hydrates or escapes at the seafloor. A variety of mechanisms are currently under investigation to determine how free gas pass through the gas hydrate stability zone. Gas may migrate through fractures or along tensional faults, in which all water is trapped in the gas hydrates, or gas hydrate formation may be inhibited by capillary forces or by localized high salinity zones. The free gas stream may move upwards very fast up to an area where conditions are favorable to form gas hydrates. Hydrate formation may plug up the migration conduits, and as high gas pressure builds up, the gas may be rerouted into soft sediment layers. The dynamic processes that interact with a complicated plumping system may be responsible for the large variety of gas hydrate and sediment fabrics observed.

Macroscopic hydrate fabrics deeper within the stability zone are very different from the near-surface deposits because at depth hydrate formation is constrained by the pore space in which hydrate precipitates. Abegg et al. (submitted) have investigated whole-round sediment samples from hydrate intervals, which were frozen in liquid nitrogen immediately after recovery. Nearly 60 frozen hydrate samples, covering a wide depth range of the gas hydrate occurrence zone (GHOZ) of southern Hydrate Ridge, were investigated by X-ray computerized tomography (CT). All sub-surface hydrate samples appear as veins or veinlets with dipping angels of more than 30° up to vertical dipping. Such hydrates are clearly precipitates filling tectonic fractures and/or faults deeper in the sediments (Fig. 14.12), where the geo-mechanical properties of the sediment preclude massive hydrate formation. These structures are in clear contrast to those of the gas hydrate that outcrops at the seafloor (Fig. 14.11).

14.4 Pore Water Anomalies Associated with Gas Hydrate Formation and Decomposition

Gas hydrate formation involves the removal of water molecules from the surrounding pore water, as they are sequestered in the clathrate lattice. Removal of water, with the exclusion of the dissolved ions, leads to changes in the concentration of salts in the pore water. Because chloride is an abundant and usually conservative ion in pore waters of shallow marine sediment, changes in dissolved chloride content are

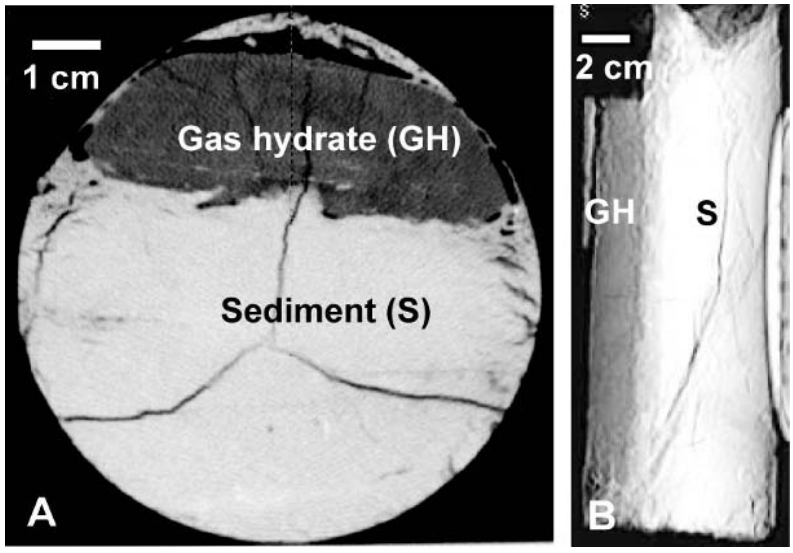

Fig. 14.12 CT-images of a core section at 87 m below sea-floor (ODP Site 1248 from Hydrate Ridge) showing that gas hydrate is filling a vertical fracture (low density is displayed in dark and high density is shown by lighter colour). A: CT-slice through the core B: CT-overview of the core section documenting the dipping of the hydrate-filled fracture parallel to the core (from Abegg et al. subm.).

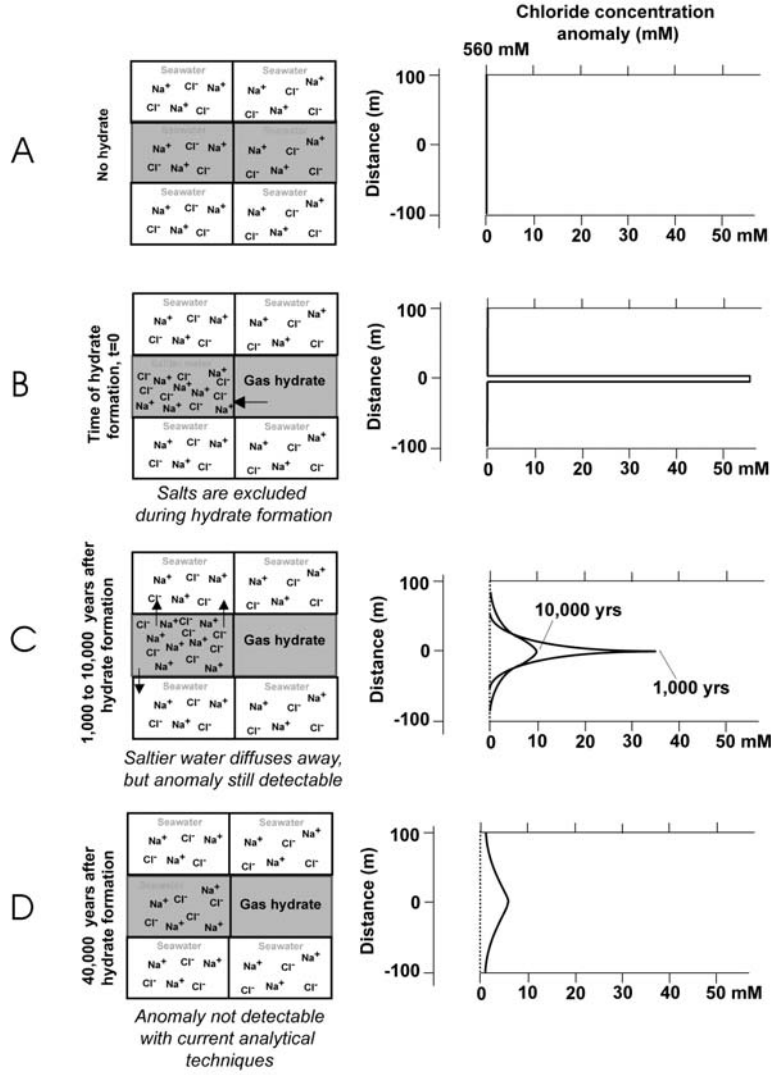

Fig. 14.13 Cartoon illustrating how gas hydrate formation increases the salinity of the adjacent interstitial pore fluid, and subsequent dissipation of the chloride anomaly via diffusion over time. A. Shows system before hydrate formation, sodium and chloride ions homogeneously distributed in the pore fluid. B. When gas hydrate forms, ions are excluded from the crystal lattice, and the pore fluids become saltier at the foci of hydrate formation. Right panel illustrates a 56 mM anomaly created by formation of gas hydrate that occupies 9% of the pore space. C. Over time the excess ions diffuse away, as illustrated by the diffusional decay model showing dissolved chloride profiles at 1,000 and 10,000 years. D. After 100,000 years, the chloride anomaly is smaller than that which can be detected with current analytical techniques. The 1-dimensional model assumes that the half width of the concentration spike to be 5 meters, a sediment porosity of 50% and the free solution diffusion coefficient for the chloride ion of 1.86 x 10^{-5} cm^2s^{-1} at 25 ^oC (modified from Ussler and Paull 2001).

commonly used to monitor formation and decomposition of gas hydrate deposits. In addition, formation of the hydrate lattice results in preferential uptake of the heavy oxygen and hydrogen atoms in the solid phase, with consequent depletion in the pore water. These two pore water parameters: dissolved chloride and the isotopic composition of the water itself, have been widely used to identify and quantify hydrate distribution and the dynamic processes involved in formation and destabilization of these deposits.

14.4.1 Gas Hydrate and Chloride Anomalies

The "Ion Exclusion" Effect

It has long been recognized that the formation and decomposition of gas hydrate lead to changes in dissolved chloride concentration of marine pore fluids (e.g. Hesse and Harrison 1981). Gas hydrates, like normal ice, exclude salts from the crystal structure, thus increasing the salinity

of the surrounding water. The change in interstitial ion concentration resulting from this "ion exclusion" mechanism is proportional to the amount of gas hydrate that is formed. Ussler and Paul (2001) use a simple cartoon to represent the effect on pore water salinity at the foci of gas hydrate formation (Fig. 14.13). They further modelled the diffusive attenuation of the chloride anomaly over time, and showed that a positive anomaly of 56 mM (created by formation of hydrate that occupies ~9% of the pore space) will not be detected with current analytical methods after about 40,000 years (Fig. 14.13).

Various numerical models have shown that generating gas hydrate to a concentration of ~10% of the pore space, in both passive and active settings (e.g. Blake Ridge, Hydrate Ridge; Nimblett and Ruppel 2003) probably required formation times of at least 10^3, and perhaps as much 10^6 years. Therefore, if chloride behaved conservatively, the pore water in contact with these deposits should have a chloride concentration similar to seawater. This is, however, not commonly the case. Indeed, fluids with chloride concentration significantly lower than seawater have been sampled from most convergent margins and such "freshening" has been attributed to gas hydrate dissociation and dehydration of hydrous minerals at depth (e.g. Gieskes et al. 1990; Kastner et al. 1991). The issue of background chloride concentration, and an example of a chloride ano-maly created by natural gas hydrate dissociation is described in the following sections.

In situ chloride concentration in pore fluids of hydrate-bearing sediments also show enrichments relative to seawater in some natural systems. These occur when the geological setting supports formation of brines, or when gas hydrate forms so rapidly that the resulting excess ions do not have sufficient time to diffuse away. These scenarios are also discussed below.

Estimating Gas Hydrate Abundance Using Dissolved Chloride Data

Because gas hydrate is not stable at the temperature and pressure conditions that exist at the sea surface, most estimates of the in situ distribution and concentration of gas hydrate rely on a variety of proxies. Perhaps the most widely used of these proxies is based on the accurate measurement of dissolved chloride in the pore fluids. During core recovery, gas hydrate dissociates, resulting in dilution of the chloride concentration by addition of water sequestered in the gas hydrate lattice prior to core recovery. The negative chloride anomalies relative to in situ chloride concentrations are proportional to the amount of gas hydrate in a sediment sample. Uncertainties in the estimates of gas hydrate abundance using the dissolved chloride proxy arise from a paucity of information on (1) the in situ dissolved chloride values, (2) the chloride content potentially trapped within the pores of the gas hydrates, and (3) the spatial sampling resolution.

There is to date no reliable data on the amount of Cl^- sequestered by the hydrate cage because the physical separation of the water released by natural hydrate dissociation from pore water contamination can be very difficult. Suess et al. (2001) suggest that there may be residual chloride trapped within the hydrate pore space. Nevertheless, since this number is small and very poorly defined, most estimates of hydrate abundance in marine sediments assume that hydrate formation excludes all dissolved ions.

If the amount of chloride ions trapped in the hydrate structure is assumed to be negligible, the measured chloride concentration after hydrate dissociation can be related to the hydrate abundance by the following equation (see Ussler and Paull 2001 for derivation).

$$Cl^-_s/Cl^-_o = 1-[V_h/(w-V_h(w-1))] \quad (1)$$

where Cl^-_s is the chloride concentration in the sample (i.e. after hydrate decomposition), Cl^-_o is the pore water concentration in situ (prior to decomposition), V_h is the volume fraction of hydrate filling pore space, and w represents the occupancy-density characteristics of the gas hydrate formed, as calculated from:

$$w = \rho_w M_h/(\rho_h M_w m_w) \quad (2)$$

Here, ρ_w and ρ_h are the densities of fresh water and gas hydrate respectively, and m_w is the number of moles of fresh water contained in 1 mole of gas hydrate. M_w and M_h represent the molecular weights of water and gas hydrate, respectively. The value of M_h depends on the degree of occupancy of the hydrate structure. When the structure is fully occupied, 1 mole of gas hydrate contains 5.9 moles of water, its density is 910 kg m^{-3} and its molecular weight is 122.2 g mol^{-1} (Ussler and Paull 2001).

The use of the chloride proxy is predicated on the assumption that the background chloride concentration is known and that the rate of hydrate formation

is slow enough that high chloride anomalies resulting from salt exclusion during hydrate formation have been removed by diffusion and advection. A recurrent issue in these studies is the need for a robust estimate of the background chloride values (Cl_o in equation 3) against which the anomalous discrete excursions can be calculated.

Ussler and Paull (2001) nicely illustrate the effect that selecting various values for Cl_o has on the estimate of gas hydrate concentration, by comparing two approaches for estimating pore water baselines (Fig. 14.14). Using examples from a passive (Site 997, Blake Ridge) and active margin (Site 889, northern Cascadia margin), they clearly illustrate that simply assuming seawater dissolved chloride values as a baseline against which to measure the degree of dilution, in most cases will give wrong results. The smoothed baseline approach produces an estimate of gas hydrate more consistent with other independent hydrate proxies, and with the phase change that occurs at the bottom of the GHSZ. To construct robust estimates of the hydrate abundance based on the dissolved chloride proxy, it is important to understand the processes that affect the in situ chloride distribution at each location.

The low chloride values measured below the BSR at sites drilled on the Blake Ridge (passive margin setting) have been attributed to long-term hydrate melting below the gas hydrate stability zone. A more pronounced freshening is observed in pore waters from active margin settings, as observed at Sites 889 in the northern Cascadia margin (Fig. 14.14), and in the Middle America trench at Sites 497, 498 (Harrison and Curiale 1982) and 568 (Hesse et al. 1985). It was unclear, though, if this deep freshening effect was due to gas hydrate processes or to other reactions independent of hydrate formation (Ussler and Paull 2001).

Data generated by drilling along an east-west transect in the southern Hydrate Ridge region

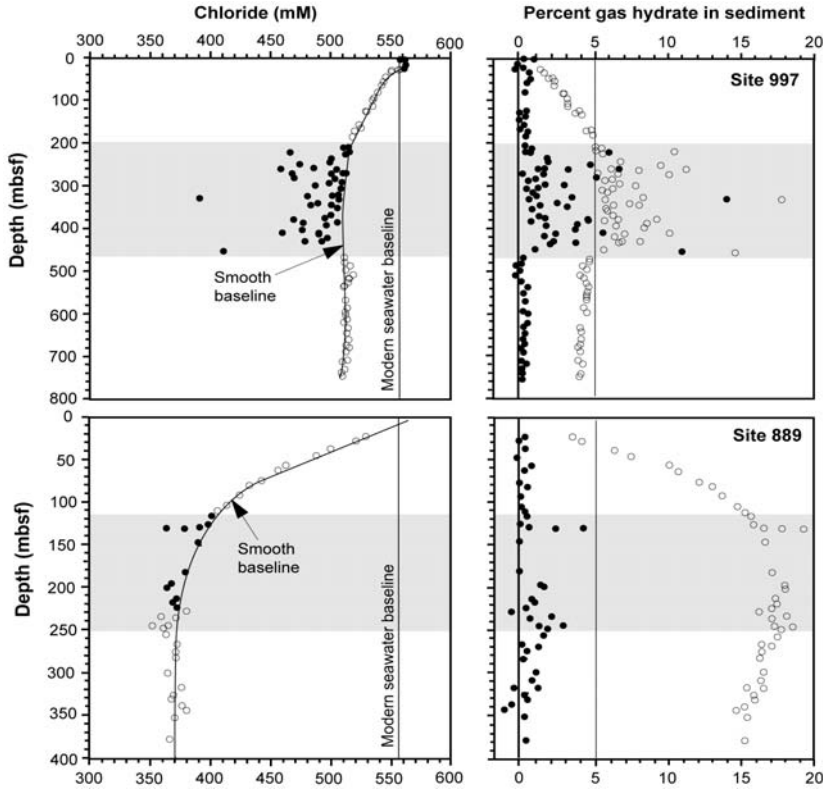

Fig. 14.14 Comparison of estimates of hydrate concentration based on two approaches for estimating the background chloride concentration (Cl^-_o in equation 3). Upper panel uses data from a passive margin (Site 997, Blake Ridge) and bottom panel shows data collected at an active margin (Site 889, northern Cascadia margin). In both cases, the shaded area denotes the region where gas hydrate is believed to be present, and the BSR denotes the geophysical reflector that indicates the bottom of the gas hydrate stability zone. The use of a modern seawater baseline predicts much larger amounts of gas hydrate, and suggests the presence of gas hydrate below the GHSZ (from Ussler and Paull 2001).

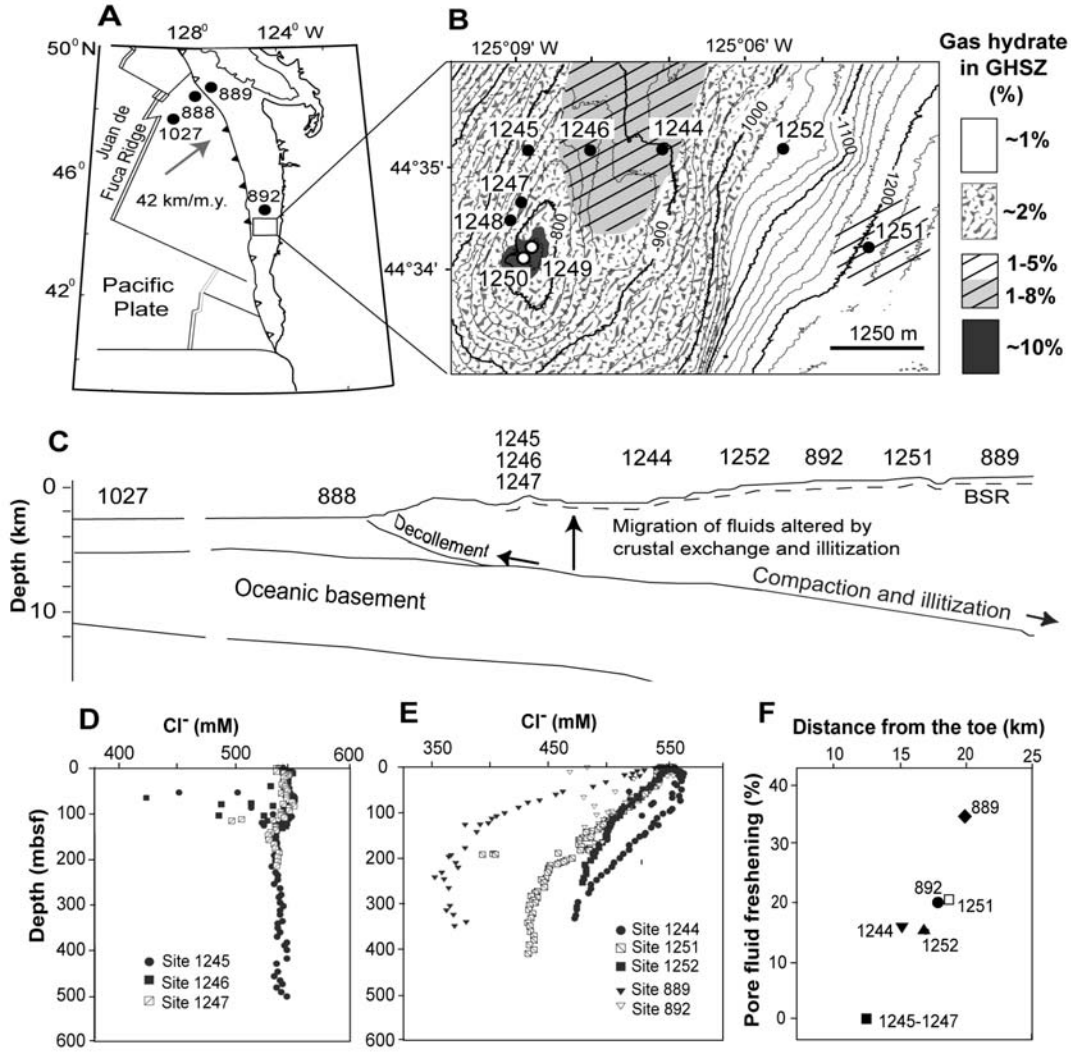

Fig. 14.15 Chloride freshening due to progressive illitization along the Cascadia margin accretionary margin. A. Tectonic setting. B. Details of sites drilled during ODP Leg 204, showing the gas hydrate distribution. C. Location of the sites relative to a schematic transect arcward from the incoming plate, the relative site locations are not to scale. D. Dissolved chloride at sites drilled less than 10 km away from the toe of the prism, showing no significant freshening at depth. Gas hydrate is apparent in discrete anomalies in the GHSZ. E. Freshening of deep fluids from sites drilled at various distances from the prism toe. F. Increase in pore fluid freshening of mélange samples with distance from the prism toe, consistent with progressive illitization as mélange sequences are exposed to higher temperatures over longer time periods (Figure modified from Torres et al. 2004).

has recently shown the separate effects of clay dehydration reactions and gas hydrate dissociation on the dissolved Cl^- distribution. These data provide geochemical evidence to evaluate the baseline question, and provide an example of a system where hydrate is present and background chloride contents do not deviate significantly from seawater values (Torres et al. 2004). As shown in Fig. 14.15, Sites 1244 and 1245 both have very similar gas hydrate contents, averaging 2-4 % within the gas hydrate stability zone, and concentrated in patchy zones that contain up to 20 % hydrate (Tréhu et al. 2004). These two sites, however, have highly different chloride baselines (Fig. 14.15). In addition, there is very little gas hydrate presence at Site 1252, as evidenced by various proxy measurements, including chloride data (Tréhu et al. 2004a), even though the trend to low chloride values is well defined at this site.

The observed freshening with depth and distance from the prism toe is consistent with enhanced conversion of smectite to illite, driven by increase in

temperature and age of accreted sediments (Fig. 14.15). Whereas discrete negative anomalies within the GHSZ are indeed the result of gas hydrate dissociation during core recovery, the smooth decrease with depth is independent of gas hydrate processes, and instead reflects the degree of illitization at depth. These results indicate that the smooth decrease with depth, commonly observed at sites drilled over accreted mélanges, is not directly related to gas hydrate abundance. Instead, chloride anomalies associated with gas hydrate should be calculated from discrete excursions to negative values against a background defined by the envelope of the measurements. In order to confidently define the dissolved chloride background concentration, care should be taken in obtaining enough resolution of the pore fluid sampling.

The presence of negative "spikes" in the chloride distribution suggests that the distribution of gas hydrate in marine sediments is highly heterogeneous. Whereas some observations reveal association of hydrate with coarse, high porosity horizons (Clennell et al. 1999), the factors controlling distribution of gas hydrate are not fully understood. Nevertheless, the question remains as to whether the patchy distribution of these deposits can be adequately mapped with pore water analyses. Limitations on how much pore water can be extracted from a section of the core, how many core sections can be dedicated to these analyses, and the time needed for each measurement, usually only allow for sparse measurements of the pore water composition.

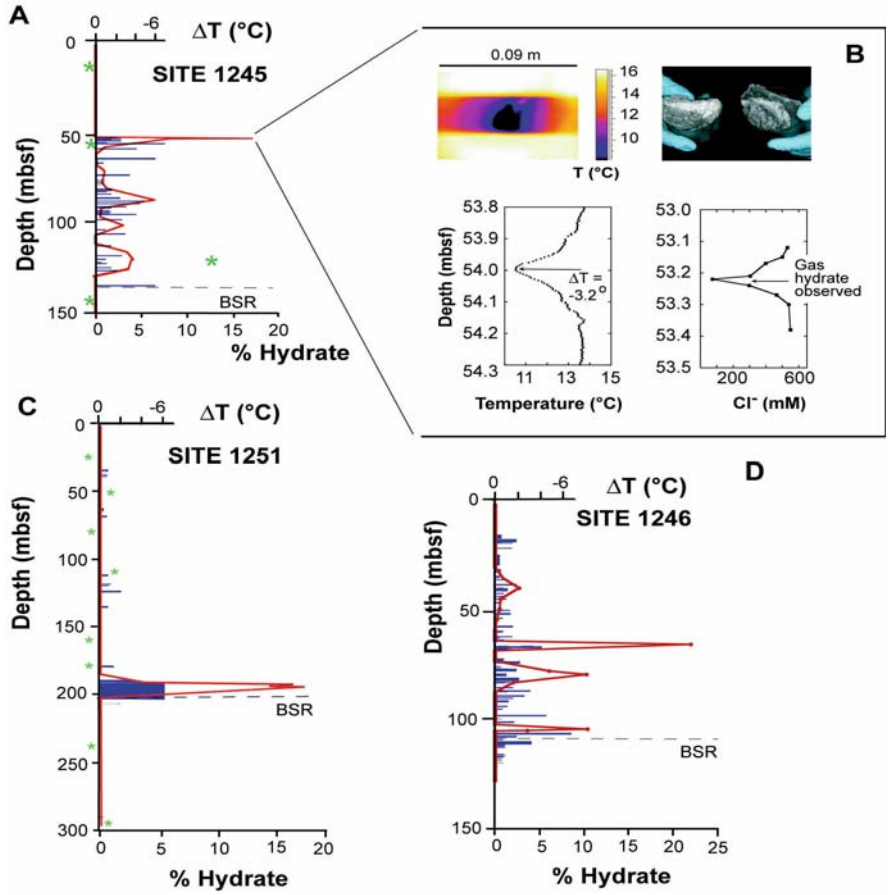

Fig. 14.16 Comparison of ΔT anomalies (blue lines) to gas hydrate content estimated from discrete anomalies in the dissolved chloride distribution (red lines), and given as percent occupancy of the pore space, for 3 sites drilled during ODP Leg 204. Green lines denote estimates based on data from pressure core barrel deployments. Horizontal (dashed) lines denote the depth of seismic reflectors corresponding to the bottom of the GHSZ (BSR). Location of the sites is shown in Figure 11. Insert B shows the temperature profile derived from an infrared image in the vicinity of a 2 cm-hydrate layer recovered from Site 1245, and the corresponding chloride concentration in closely-spaced pore water samples. The apparent offset in depth between the two graphs is due to the removal of core as gas expansion voids between the time when the IR data was collected and the pore water samples were taken (modified from Tréhu et al. 2004a).

Typical deep-sea drilling sampling resolution is on the order of one sample every 3 to 10 meters.

Other proxies have been developed to produce a more continuous, high resolution record of hydrate distribution in marine sediments. Among these, the use of an infrared (IR) camera to map cold spots in the core resulting from the endothermic decomposition of gas hydrate has proven to be highly effective (e.g. Weinberg et al. 2005). However the absolute value of the temperature measured by the IR camera depends on many different variables, including time of day, core depth and coring technique (Tréhu et al. 2003), and plots of temperature along the core are very noisy. A simple way of parametizing and displaying the IR temperature data is to define ΔT as the temperature anomaly relative to the local background. High-resolution measurements of chloride anomalies in core sections previously imaged with an IR camera can provide a calibration function needed to correlate the temperature anomaly with hydrate content, as shown in Figure 14.16B. These data, not only provide a means of calibrating the temperature anomalies, but also illustrates how a discrete hydrate layer can be easily missed with coarse sampling resolution. Samples collected from a 2-cm-thick hydrate layer and as much as 5 cm away from it show significant anomalies in the chloride content, whereas samples collected at distances >10 cm from the hydrate layer do not show any deviation from the background chloride values (Fig. 14.15).

Whereas the dissolved chloride measurements alone may not fully constrain the gas hydrate distribution, the good correlation between dissolved chloride and temperature anomalies shown in Figure 14.16 (Tréhu et al. 2004a), gives support to the use of a combined ΔT-ΔCl approach to best define an heterogeneous hydrate distribution. An understanding of the spatial variability in gas hydrate distribution may provide valuable insights into the possible response of these deposits to tectonic and environmental change.

Gas Hydrate Destabilization via Natural Processes

If environmental changes induce gas hydrate dissociation, the negative anomaly associated with water release would be attenuated over time by diffusion processes. The mathematical treatment of the signal attenuation is analogous to that described above for hydrate formation. An example of the chloride attenuation from natural dissociation processes on Hydrate Ridge is described by Bangs et al. (2005). These authors explain the presence of a double BSR in the seismic records as a remnant of a BSR_S that probably formed during the last glacial maximum

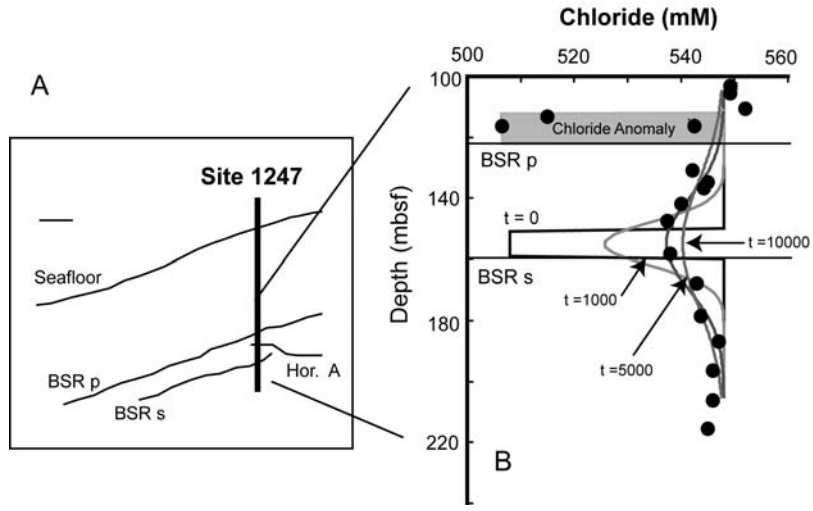

Fig. 14.17 A. Diagram illustrating the double BSR observed in seismic data in the vicinity of Site 1247. B. Chloride concentration in pore waters from site 1247, compared with expected values derived from a diffusive attenuation model following gas hydrate dissociation. The assumed hydrate content at time zero has a width of 10 m and a magnitude comparable to the anomaly observed just above the present BSR (BSRp). The data suggest that the hydrate dissociation occurred 5000 yrs ago. The authors postulate that pressure and temperature changes in the period of 8000 to 4000 years ago, led to a shift in the depth of the hydrate stability zone, creating the double BSR (modified from Bangs et al. 2005).

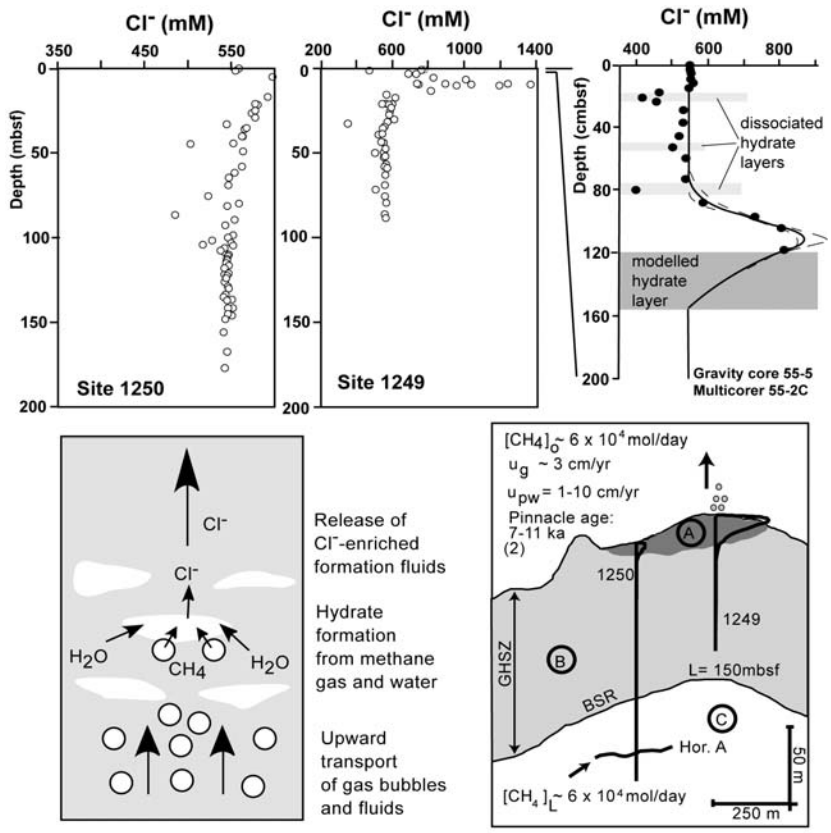

Fig. 14.18 Upper panel illustrates dissolved chloride concentration in pore waters collected from the summit of Hydrate Ridge during ODP leg 204 (Sites 1249, 1250, from Torres et al. 2004) and from a gravity core recovered from this area during RV SONNE expedition SO-143 (Haeckel et al. 2004). These data (panels A-C) indicate that hydrate is forming at very fast rates, so as to maintain the extremely high chloride values. Furthermore, to sustain the rapid formation rates, Torres et al. (2004) and Haeckel et al. (2004) show that methane must be supplied in the gas phase, as illustrated by the cartoon in panel. Methane solubility in seawater is too low for aqueous transport to deliver sufficient methane to form the observed hydrate deposits. D. Mass balance calculations based on a simple box model (E) indicate that the massive deposits recovered from the Hydrate Ridge summit probably formed in a period of the order of 100's to 1000's of years, highlighting the dynamic nature of these near-surface deposits (modified from Torres et al. 2004 and Haeckel et al. 2004).

(18,000 years ago). An increase in temperature of 3.3 °C that followed the last glaciation will shift of the hydrate stability by ~140 meters, which coupled with a concomitant sea-level rise of ~120 meters, results in an approximate net shift of the hydrate stability horizon of ~20 meters (Bangs et al. 2005). Among other evidence, the authors use a diffusion driven attenuation of the freshening signal induced by hydrate dissociation when the GHSZ shifted to a shallower depth. They show that the observed dissolved chloride distribution at a site drilled through the double BSR is consistent with a BSR shift that occurred 4,000 to 8,000 years ago (Fig. 14.17). This time frame, when analyzed in the context of thermal propagation lag in the sediment section and potential lag due to latent heat needed to dissociate hydrate, is consistent with P/T changes in the water column that occurred at the end of the LGM (Bangs et al. 2005). A shift of the depth of hydrate stability associated with post-glaciation P/T changes, has also been suggested by others for Northern Cascadia (Westbrook et al. 1994), southwestern Japan (Foucher et al. 2002) and the Norwegian margin (Mienert et al. 1998).

Pore Water Brines

In the large body of gas-hydrate bearing locations drilled to date, the dissolved chloride show lower than seawater values (see reviews by Ussler and Paull 2001; Hesse 2003). However, there are examples of gas hydrate bearing sites in which the dissolved chloride in the pore fluids is

higher than that of seawater. Most commonly these brines are associated with regions where the presence of old evaporites (e.g. Milano Dome, ODP Site 970 in the eastern Mediterranean, DeLange and Brumsack 1998), or salt-diapir intrusions (e.g. Blake Ridge Diapir ODP Site 996, Egeberg and Dickens 1999; mud volcanoes in the Northern Gulf of Mexico, Ruppel et al. 2005) leads to the enhanced chloride content. In addition to these settings, high dissolved chloride concentration associated with hydration reactions in the vicinity of an active spreading ridge was reported from ODP Sites 859 and 860 in the accretionary wedge at the Chile Triple Junction (Froelich et al. 1995).

In contrast to these regions in which brines are produced by geological processes, at the Hydrate Ridge summit, the high chloride brines observed (Haeckel et al. 2004; Torres et al. 2004) are generated by the rapid formation of gas hydrate deposits near the seafloor (Fig. 14.18). A one-dimensional transport-reaction model was used to simulate this chloride enrichment and place constrains on the mechanisms and time frames necessary to produce the observed concomitant massive hydrate deposition at the ridge summit. The models of Torres et al. (2004) and Haeckel et al. (2004) demonstrate the need for the presence of a fluid-gas mixture through the GHSZ, since the observed chloride enrichment cannot be generated exclusively from the transport of methane dissolved in the pore fluids. These massive hydrate deposits are forming very rapidly, and the continuous supply of methane gas maintains the pore water brines and the shallow gas hydrate deposits in contact with the methane-poor bottom seawater.

14.4.2 Gas Hydrate and Water Isotope Anomalies

The water sequestered in the hydrate lattice is preferentially enriched in ^{18}O and deuterium (D), thus the isotopic composition of the water in the pore spaces collected from gas hydrate bearing sediment can provide additional information on the abundance and the characteristics of these deposits. Pore fluid samples that had been modified by hydrate decomposition upon core recovery during ODP Legs 146 (Kastner et al. 1998), and 164 (Matsumoto and Borowski 2000) provided the first field data to derive the oxygen isotope fractionation factor for in situ hydrate formation. A more comprehensive sampling protocol was subsequently conducted during Leg 204 (Tomaru et al. submitted). These calculations are based on the percent variation of Cl^- relative to background (ΔCl^-):

$$\Delta Cl^- = (1 - f) \times 100 \quad (3)$$

where f is a fraction of formation water in sampled water given by:

$$f = \frac{Cl^-_S}{Cl^-_0} \quad (4)$$

Cl^-_S and Cl^-_0 are the Cl^- concentrations of sampled and formation water (i.e., in situ interstitial water) determined as background, respectively. The fractionation factors for oxygen (α_O) and hydrogen (α_H) can be determined from equilibrium equation, such that:

$$\Delta\delta = \delta_{GH} - \delta_0 = 1000 \cdot \ln\alpha \cdot (1 - f) \quad (5)$$

where α_{GH} and α_0 are is $\delta^{18}O$ or δD values for gas hydrate and formation (background) water.

Figure 14.19 illustrates how the fractionation of ^{18}O to ^{16}O and H to D between pore water, and water derived from hydrate dissociation is related to the fractionation under in situ conditions, assuming a closed system. The average values of α_O and α_H from Leg 204 samples with negative ΔCl^- are calculated to be 1.0025 and 1.022. These fractionation factors agree with previously estimated α_O values from Leg 146 (Kastner et al. 1998) and Leg 164 (Matsumoto and Borowski 2000), and with the extrapolated α_H value from Leg 112 (Kvenvolden and Kastner 1990).

Figure 14.19 illustrates the fractionation factors for in situ hydrate formation that correspond to experimentally obtained values for oxygen (α_o: 1.0023 to 1.0032) and for hydrogen (α_H :1.014 to 1.022) (Maekawa 2004). Analyses of pore water samples from a pore water brine sampled during Leg 204 reveal the oxygen and hydrogen isotopic fractionation during hydrate formation in natural systems. There are special challenges in fully constraining these values, since the dissolved chloride data from these brines reflects a mixture of the in situ fluids, with an unknown amount of fresh water added by hydrate dissociation during sample recovery. Nevertheless, Tomaru et al. (submitted) show that the isotopic fractionation in these massive deposits departs significantly from experimental data. More research is needed to fully understand these deviations.

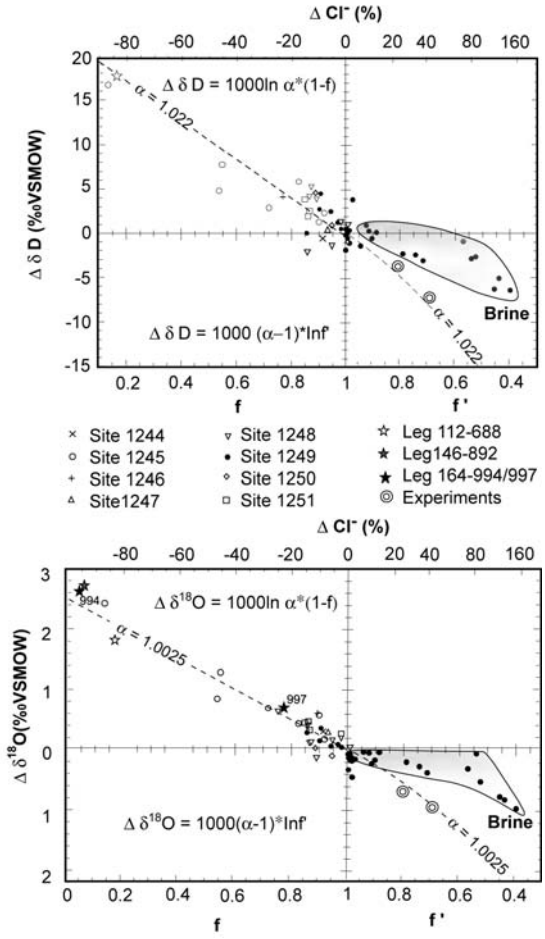

Fig. 14.19 Isotopic fractionation between water in the pore fluid and water in the hydrate lattice as a function of chloride anomalies (ΔCl). Hydrate dissociation causes chloride dilution and ^{18}O, D enrichment. The fractionation factors α_0 = 1.0025 and α_H = 1.022 are based on data from low-chloride pore waters recovered from Hydrate Ridge during ODP Leg 204. They are in agreement with previous estimates from Legs 146 and 164, as well as with experimentally determined values during hydrate formation shown by open circles. Samples collected from pore water brines deviate considerably from expected values (from Tomaru et al., submitted).

14.5 Gas Hydrate Carbonate Formation and Anaerobic Oxidation of Methane

14.5.1 Petrographic Characteristics of Clathrites

Authigenic carbonates are common features at seafloor seepage sites where fluids enriched in methane or oversaturated in bicarbonate escape from seafloor. Various investigators have described a particularly large variety of carbonates from the Cascadia margin (Kulm et al. 1986; Ritger et al. 1987; Sample and Reid 1998; Greinert et al. 2001). Detailed petrographic, mineralogical and isotopic work was performed on a wide collection of samples that document several petrographically distinct lithologies. Carbonates occurr in boulder fields or in massive autochthonous chemoherm complexes (Teichert et al. 2005a). Other carbonates were sampled in direct contact with hydrates and in others, a direct relationship to gas hydrates was recognized (Bohrmann et al. 1998; Teichert et al. 2004). There are two main lithologies: a breccia composed of micrite-cemented monomict clasts, and pure aragonite of various appearances.

The breccia show angular clasts composed of the same fine-grained material as the terrigenous soft sediment on the seafloor, and submicrometer anhedral Mg-calcite crystals have been observed in the intergranular pore space between the terrigenous components (Bohrmann et al. 1998; Greinert et al. 2001). Although the grain-supported texture (Figs. 14.20A and 14.20B) shows up to 20-30% pore space, the clasts do not appear to have been transported over longer distances. The breccia is thought to form by the collapse of the clasts when gas hydrate in the sediment dissociates, followed by cementation with Mg-calcite and aragonite.

The second obvious carbonate lithology is composed of aragonite precipitates, that appear either as pure isopachous fringe cements (Fig. 14.20B) or as yellow layers of remarkable purity (Figs. 14.20A, 14.20C, and 14.20E). Pieces of isolated yellow aragonite layers have often been found associated with gas hydrates. Such layers have variable thicknesses of 1 to 3 cm, occur often in pieces of 10 to 20 cm in diameter and reveal truncated edges. The continuous aragonite layers grow directly within pure gas hydrate layers parallel to stratification and are therefore free of terrigenous sediment impurities. In several cases the aragonite precipitates have been directly recovered from within pure gas-hydrate layers (Greinert et al. 2001). The precipitates often exhibit a shape that partially images the inner surface morphology of the gas hydrate bubble fabric (Fig. 14.20E).

Such gas hydrate carbonates are also called clathrites and form archives in which geochemical processes of clathrate and clathrite formation is well documented (Teichert et al. 2005b). Their carbon isotope values range from -40‰ to -54‰ PDB, identifying methane as the dominant carbon source (Fig. 14.21). Bohrmann et al. (1998) analyzed mixtures of Mg-calcite and aragonite and showed that their oxygen isotopic composi-

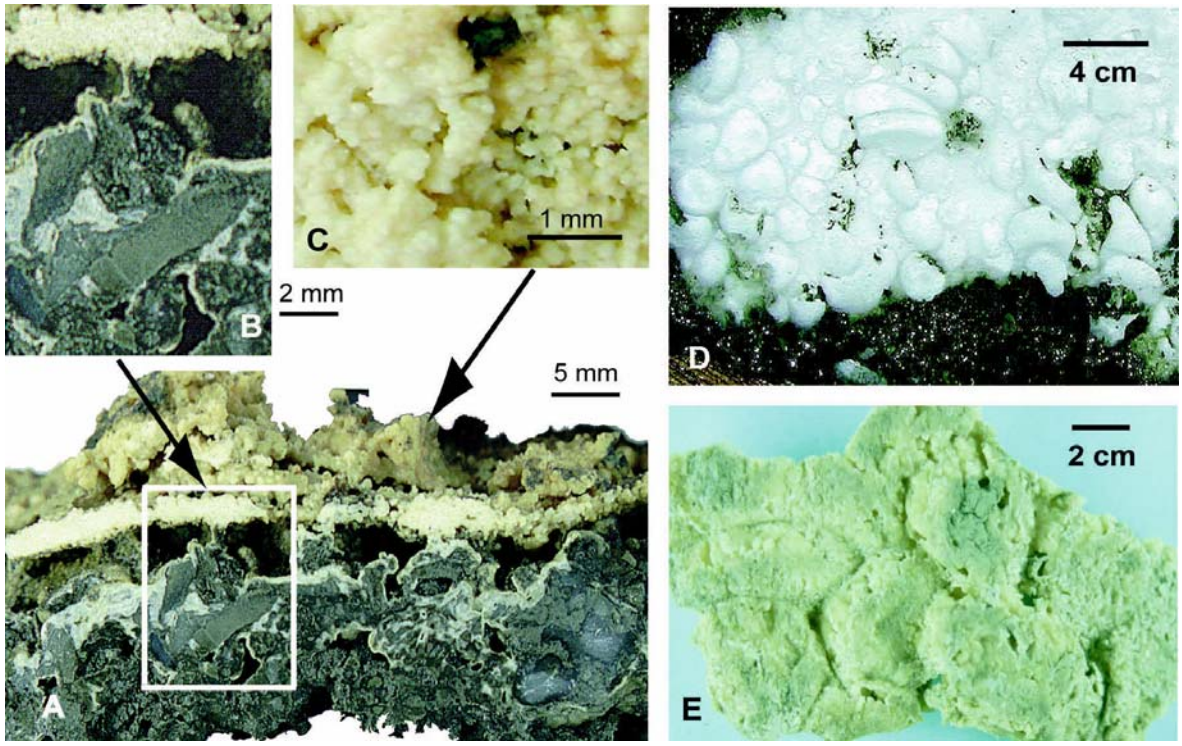

Fig. 14.20 (A) Vertical section trough an authigenic carbonate layer, showing a continuous aragonite (light) layer and fringe cements around Mg-calcite-cemented clasts. (B) Detail of the breccia. (C) Botryoidal features from the surface of the pure aragonite layer. (D) Bubble fabric of a pure methane hydrate layer and (E) corresponding aragonite layer imaging the bubble structure.

tion varies as a function of mineralogy (Fig. 14.21). The $\delta^{18}O$ value of the aragonite end-member (+3.68‰ PDB) is lower than the $\delta^{18}O$ of Mg-calcite (+4.86‰ PDB). By using appropriate isotope fractionation equations for each mineral, Bohrmann et al. (1998) calculated the oxygen isotopic composition of the pore water from which the carbonates precipitated. They found that the aragonite incorporates the isotopic composition of standard mean ocean water (SMOW) under recent seafloor conditions, when gas hydrates are also forming. In contrast, Mg-calcite most likely precipitated in response to destabilization of gas hydrates, because the pore water from which Mg-calcite precipitated is enriched in ^{18}O relative to SMOW. Similar associations have since been documented for authigenic carbonate recovered from the Gulf of Mexico (Formolo et al. 2004), further establishing that these minerals are valuable records of gas hydrate formation and destabilization through geologic time.

14.5.2 Carbonate Precipitation through Microbial Activity

Methane from gas hydrates greatly stimulates the entire ecosystem at cold seeps. (Suess et al. 2001, Sahling et al. 2002). On the basis of quantitative analyses of pore water sulfate and methane profiles, corroborated by isotopic mass balance models, geochemists postulated the anaerobic oxidation of methane (AOM) via sulfate reduction, as a dominant microbial process at cold seeps. (Suess and Whiticar 1989; Borowski et al. 1999), However, the AOM remained controversial for several years because the microbes responsible for this reaction proved to be very elusive. Only recently was a microbial consortium of methanotrophic archaea and sulfate-reducing bacteria identified on gas hydrate-bearing samples from Hydrate Ridge (Boetius et al. 2000). This interesting discovery was followed by similar findings on cold seeps and hydrate deposits in the Eel river basin (Orphan et al. 2004) and the Gulf of Mexico (Joye et al. 2004). These consortia consists of an inner sphere

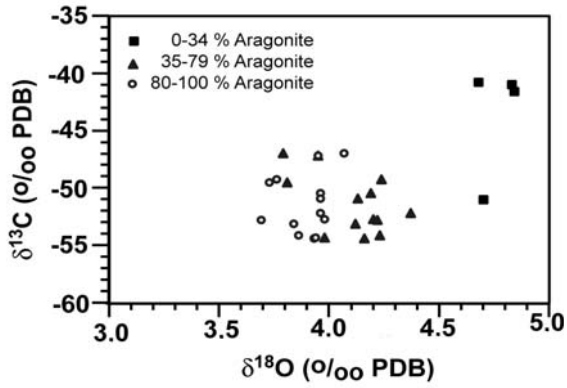

Fig. 14.21 Carbon and oxygen isotope values from gas hydrate carbonates of southern Hydrate Ridge. The carbonates are mixtures between Mg-calcite and aragonite; note the variation in oxygen isotope values with changing aragonite content (Bohrmann et al. 1998).

containing about 100 archaeal cells surrounded by about 200 cells of sulfate reducing bacteria (Fig. 14.22), and it operates via two possible separate reactions.

The archaea oxidize methane:

$$CH_4 + 2H_2O \longrightarrow CO_2 + 4H_2 \qquad (6)$$

And sulfate reducing bacteria may act in two ways, indicated by reactions (7) and (8)

$$SO_4^{2-} + 4H_2 + H^+ \longrightarrow HS^- + 4H_2O \qquad (7)$$

$$SO_4^{2-} + CH_3COOH + 2H^+ \longrightarrow 2CO_2 + H_2S + 4H_2O \qquad (8)$$

Both reaction pathways are under discussion and it is not totally clear whether hydrogen is directly consumed (equation 7) or acetate is used (equation 8), though scavenging of H_2 will enhance the effectiveness of reaction (6). The net reaction can be summarized in the following equation,

$$CH_4 + SO_4^{2-} \longrightarrow HCO_3^- + HS^- + H_2O \qquad (9)$$

The metabolic coupling involved in AOM, produces sulfide and dissolved inorganic carbon. Both methane and sulfate needed for AOM, are available in large amounts where methane vents are present at the seafloor. In the case of Hydrate Ridge, gas hydrates provide an almost inexhaustible supply of methane and the ocean water constitutes a large sulfate reservoir. Here the anaerobic methane oxidation rate is large because of the conti-nuous supply of methane from deeper sediments.

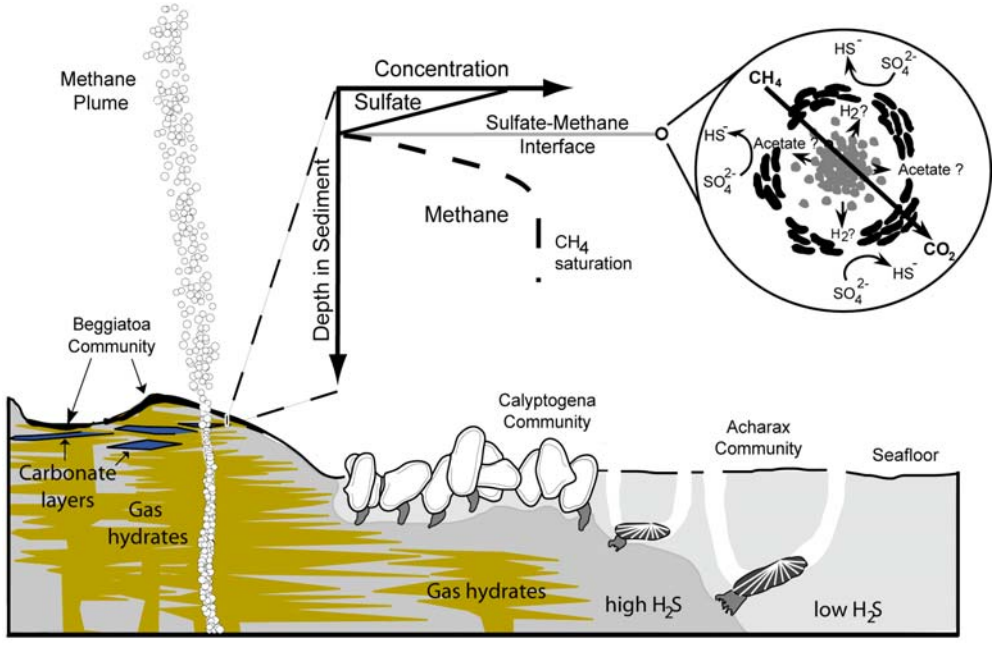

Fig. 14.22 Schematic illustration of gas hydrate deposits and biogeochemical reactions in near-surface sediments on southern Hydrate Ridge. High gradients in pore water sulfate and methane are typical of methane hydrate-rich environment close to sulfate-rich seawater. At the sulfate-methane interface (also named sulphate-methane transition in earlier chapters of the book) a microbial consortium of methanothrophic archaea and sulfate-reducing bacteria (Boetius et al. 2000) perform anaerobic oxidation of methane (AOM) leading to carbonate precipitation. AOM rates influence hydrogen sulfide fluxes and gradients, which are reflected on the seafloor by the distribution of vent communities around active gas seeps and gas hydrate exposures (Sahling et al. 2002).

The formation of hydrogen sulfide constitutes an energy source for chemoautotrophic organisms living on the seafloor. The colonization of the seeps depends on the local H_2S-gradient generated by AOM (Barry and Kochevar 1998; Sahling et al. 2002). The sulfide-oxidizing bacterium *Beggiatoa*, is usually found forming mats in areas with very high sulfide flux. *Calyptogena* clams, typically colonize areas with lower sulfide concentrations and surround the *Beggiatoa* mats. *Acharax* clams live in burrows within the sediment and are restricted to environments of very low sulfide concentration (Fig. 14.22). In addition to sulfide production, AOM increases carbonate alkalinity, which drives pervasive carbonate precipitation. The high concentration of bicarbonate as respiration product (equation 9), the presence of microbial surfaces, and the exudation of organic polymers that can bind calcium ions are all factors that support active carbonate precipitation (Iversen and Jørgensen 1985). Near-surface deposits of porous gas hydrate (Fig. 14.11) are ideal sites for AOM because sulfate can migrate through the porous space to the inner parts of the hydrates, where the microbial consortia can thrive. The aragonite precipitates observed within the sponge-like bubble structure of gas hydrates are evidence for such microbial processes. In addition, biomarker analyses of those layers show extremely high amounts of components (e.g. isoprenoids crocetane and pentamethylicosane) typical of those produced by methane-consuming and sulfate-reducing microorganisms (Elvert et al. 2001).

14.6 Concluding Remarks

Although the existence of gas hydrates has now been known for decades, our understanding of their potential impact on slope stability, the biosphere, carbon cycling, and climate change is still in its infancy. Laboratory and field studies at gas-hydrate-bearing sites, including several drilling expeditions in the past decade, have provided critical background data on the conditions of gas hydrate stability, and provide overall view of the composition and distribution of gas hydrates in nature (e.g. Dickens 2003). These results have sparked the development of models relating hydrate dynamics to tectonic and slope stability, and the possible impact of this system on global climate (Dickens 2003; Davie and Buffett 2001; Sloan 1998; Clennell et al. 1999).

Although the total amount of carbon trapped in gas hydrate is poorly constrained, existing knowledge suggest that these deposits may constitute a significant carbon reservoir, but a quantitative evaluation of its resource potential depends on reliable global and national inventories, and a better understanding of the geologic factors that lead to highly concentrated hydrate deposits.

Methane is a powerful greenhouse gas with a Greenhouse Warming Potential (GWP) 23 times that of CO_2 on a per-molecule basis. Sudden release of methane from gas hydrate therefore has the potential to affect global climate, and current hypotheses attribute past climate variations to methane release from gas hydrates in response to ocean warming and/or sea level change (Paull et al. 1991; Kennett et al. 2002; Dickens et al. 1995; Haq 1998). However, these hypotheses have yet to be confirmed and more research is needed to evaluate hydrate response to environmental change; the fate of steady fluxes of methane from hydrate reservoirs to the seabed, ocean surface and the atmosphere; and the radiative forcing of methane on climate change.

The impact of gas hydrate on seafloor stability is important for evaluating the safety of offshore structures as well as for understanding its role in rapid release of methane, which may affect climate change. Since gas hydrate encases large volumes of methane, when destabilized, these deposits may transform the host sediment into a gassy, water rich fluid. However, any buildup of overpressure from excess gas will depend on the balance between hydrate dissociation and pressure dissipation through possible permeability barriers. Freshening of the pore water may trigger slope instabilities through a possible „quick clay" behavior, which in turns would depend on the clay mineralogy of the sediment. Although massive landslide triggered by gas hydrate destabilization has not been directly observed, various investigators have shown that vast stretches of the oceanic margins where there is evidence for major large-scale slides and slumps coincide with deep water gas hydrate horizons (Mienert et al. 1998; Nisbet and Piper 1998; Paull et al. 2000). There are still gaps in our understanding of the mechanisms through which decaying hydrate may affect slope stability, on the triggering mechanism for gas hydrate decay, and on the environmental response to slope failure, in particular the possible generation of tsunamis (Driscoll et al. 2000). There are ongoing efforts to understand these phenomena and to develop predictive models, for example, in the region of the Storrega slide, off the coast of Norway (Bouriak et al. 2000; Bryn et al. 2003).

A full understanding of the complex interrelationships associated with the presence of gas

hydrate in nature requires comprehensive interdisciplinary studies that inlude laboratory experiments, numerical modelling and field observations. Because the factors that influence gas hydrate stability and the processes that occur as a consequence of gas hydrate formation are highly dynamic, these interrelationships can only be understood through time-series monitoring of complementary parameters over space and time though the installation of seafloor observatories. Efforts to establish such observatories are underway at a few key gas hydrate locations. These and other ongoing studies may well provide key answers to our current challenges of evaluating the role of these deposits in the global energy resources of the future, and on the global carbon cycle, climate change, and perhaps biotic evolution through our planet's geologic history.

Acknowledgements

This research used data provided by the Ocean Drilling Program (ODP), which is sponsored by the US National Science Foundation and participating countries under management of Joint Oceanographic Institutions (JOI), Inc. Funding for this research was provided by the U.S. Science Support Program (USSP) grant F001557, WCNURP grant PF806880 and by NSF grant OCE-9731157. The Federal Ministry of Education and Research (BMBF, Berlin) supported the studies by grant 03G0604A (collaborative project METRO). This is publication GEOTECH-194 of the program GEOTECHNOLOGIEN of the BMBF and DFG and publication No 0336 of the Research Center Ocean Margins of the University of Bremen.

14.7 Problems

Problem 1

The thermodynamically defined gas hydrate zone in sediments of the deep sea is much thicker than in sediments underlying shallow water, such as those in the upper continental slope (see Fig. 14.4). Does this mean that gas hydrate concentrations are higher in the deeper ocean than on the upper slope?

Problem 2

Discuss different methane sources in sediments. Is there a difference in hydrate formation whether the gas is biogenic or thermogenic in origin?

Problem 3

A sample collected from 90 meters below seafloor on Hydrate Ridge has an in situ methane concentration of 300 mM. Based on the phase boundary diagram shown in Fig.14.5B, do you expect hydrate to be present in this sample? If a sample with the same methane concentration was recovered from 250 mbsf, would there be hydrate in it? Why/why not. Discuss also a methane concentration of 10 mM in samples from 90 and 250 mbsf using Fig 14.5 B.

Problem 4

A water sample recovered from a gas-bearing region has a chloride concentration of 530 mM and sulfate concentration of 26.5 mM. Do you expect methane hydrate to be present?

Problem 5

Pore water samples from a hydrate-bearing core were shown to have a dissolved chloride concentration of 507 mM. If the background concentration at this site is known to be 550 mM, calculate the percent of the pore space that is occupied by gas hydrate, assuming full occupancy of the hydrate structure.

Problem 6

How could you explain the formation of shallow brines are formed in marine pore water, where there is no association with evaporites?

References

Abegg, F., Bohrmann, G., and Kuhs, W.F., subm., Data Report: Shapes and structures of gas hydrates from Hydrate Ridge imaged by CT-imaging of samples drilled during ODP Leg 204.

Bangs, N.L.B., Musgrave, R.J., and Tréhu, A.M., 2005. Upward shifts in the southern Hydrate Ridge gas hydrate stability zone following postglacial warming, offshore Oregon. J. Geophys. Res., 110:10.1029/2004JB003293.

Barry, J.P., Kochevar, R.E., 1998. A tale of two clams: Differing chemosynthetic life styles among vesicomyids in Monterey Bay cold seeps. Cahiers de Biologie Marine 39 (3-4): 329-331.

Bernard, B.B., Brooks, J.M., and Sackett, W.M. 1976. Natural gas seegage in the Gulf of Mexico. Earth and Planetary Science Letters 31(1): 48-54.

Bily, C., and Dick, J.W.L., 1974. Naturally occurring gas hydrates in the Mackenzie Delta. Bulletin of Canadian Petroleum Geology, 22: 320-352.

Boetius, A., K. Ravenschlag, K., Schubert, C.J., Rickert, D., Widdel, F., Gieseke, A., Amann, R., Jørgensen, B.B., Witte, U., and Pfannkuche, O., 2000. A marine microbial consortium apparently mediating anaerobic oxidation of methane. Nature, 407: 623-626.

Bohrmann, G., Greinert, J., Suess, E., and Torres, M., 1998. Authigenic carbonates from the Cascadia subduction zone and their relation to gas hydrate stability. Geology 26: 647-650.

Bohrmann, G., Ivanov, M.K., Foucher, J.P., Spiess, V., Bialas, J., Greinert, J., Weinrebe, W., Abegg, F., Aloisi, G., Artemov, Y., Blinova, V., Drews, M., Heidersdorf, F., Krabbenhöft, A., Klaucke, I., Krastel, S., Leder, T., Polikarpov, I., Saburova, M., Schmale, O., Seifert, R., Volkonskaya, A., and Zillmer, M., 2003. Mud volcanoes and gas hydrates in the Black Sea: new data from Dvurechenskii and Odessa mud volcanoes. Geo-Marine Letters, 23: 239-249.

Borowski, W.S., Paull, C.K., and Ussler, W., III, 1999. Global and local variations of interstitial sulfate gradients in deep-water, continental margin sediments: Sensitivity to underlying methane and gas hydrates. Marine Geology, 159: 131-154.

Bouriak, S., Vanneste, M., and Saoutkine, A., 2000. Inferred gas hydrate and clay diapirs near the Storegga Slide on the southern edge of the Vøring Plateau, offshore Norway. Marine Geology, 163:125-148.

Brewer, P.G., Franklin, M.J., Friedrich, G., Kvenvolden, K.A., Orange, D., McFarlane, J., and Kirkwood, W., 1997. Deep-ocean field test of methane hydrate formation from a remotely operated vehicle. Geology, 25: 407-410.

Brooks, J.M., II, M.C.K., Fay, R.R., and McDonald, T.J., 1984. Thermogenic gas hydrates in the Gulf of Mexico. Science, 223: 696-698.

Bryn, P., Solheim, A., Berg, K., Lien, K., Forsberg, C.F., Haflidason, H., and Ottensen, D., 2003. The Storegga Slide complex: repeated large scale sliding in response to climatic cyclicity, *in* Locat, J., and Mienert, J., (eds.), Submarine mass movements and their consequences. Advances in natural and technical hazards research, 19: 215-222.

Buffet, B., and Archer, D., 2004. Global inventory of methane clathrate: sensitivity to changes in the deep ocean: Earth and Planetary Science Letters, 227: 185-199.

Carroll, J., 2003. Natural gas hydrates - a guide for engineers: Burlington, Ma, Elsevier Science, 270 p.

Charlou, J.L., Donval, J.P., Fouquet, Y., Ondreas, H., Cochonat, P., Levaché, D., Poirier, Y., Jean-Baptiste, P., Fourré, E., Chazallon, B., and Party, T.Z.L.S., 2004. Physical and chemical characterization of gas hydrates and associated methane plumes on the Congo-Angola Basin. Chemical Geology: 205: 405-425.

Claypool, G.E., and Kaplan, I.R., 1974. The origin and distribution of methane in marine sediments, *in* Kaplan, I.R., ed., Natural gases in marine sediments, pp. 99-139.

Claypool, G.W., and Kvenvolden, K.A., 1983. Methane and other hydrocarbon gases in marine sediments: Ann. Rev. Earth Planetary Science, 11: 299-327.

Clennell, M.B., Hovland, M., Booth, J.S., Henry, P., and Winters, W.J., 1999. Formation of natural gas hydrates in marine sediments, 1, Conceptual model of gas hydrate growth conditioned by host sediment properties: Journal of Geophysical Research, 104: 22985-23003.

Clennell, M.B., Judd, A., and Hovland, M., 2000. Movement and accumulation of methane in marine sediments: Relation to gas hydrate systems, *in* Max, M.D., ed., Natural Gas Hydrate in Oceanic and Permafrost Environments: Dordrecht, Kluwer Academic Publ., pp. 105-122.

Collett, T., 2002. Energy resource potential of natural gas hydrates: AAPG Bulletin, 86: 1971-1992.

Colwell F., Matsumoto R., Reed D., 2004. A review of the gas hydrates, geology, and biology of the Nankai Trough. Chemical Geology, 205 (3/4): 391-404.

Davie M.K. and Buffett B.A., 2001. A numerical model for the formation of gas hydrate below the seafloor Journal of Geophysical Research, 106B (1): 497-514.

Davie, M.K., and Buffett, B.A., 2003. Sources of methane for marine gas hydrate: inferences from a comparison of observations and numerical models. Earth and Planetary Science Letters, 206: 51-63.

Davis, E.E., Hyndman, R.D., and Villinger, H., 1990. Rates of fluid expulsion across the Northern Cascadia accretionary prism: Constraints from new heat flow and multichannel seismic reflection data. Journal of Geophysical Research, 95: 8869-8889.

Davy, H., 1811. On a combination of oxymuriatic gas and oxygen gas: Philosophical Transactions of the Royal Society, 155 pp.

De Graaf, W., Wellsbury, P., Parkes, R.J., and Cappenberg, T.E., 1996. Comparison of acetate turnover in methanogenic and sulfate-reducing sediments by radio- and stable-isotope labeling and specific inhibitors: evidence for isotopic exchange. Appl. Env. Microbiol., 62: 772-777.

De Lange, G.J., and Brumsack, H.-J., 1998. The occurrence of gas hydrates in Eastern Mediterranean mud dome structures as indicated by pore-water composition, *in* Henriet, J.P., and Mienert, J., eds., Gas Hydrates: Relevance to World Margin Stability and Climate Change, Special Publications, 137: London, Geological Society, pp. 167-175.

Dickens, G.R., and Quinby-Hunt, M.S., 1994. Methane hydrate stability in seawater: Geophysical Research Letters, 21: 2115-2118.

Dickens, G.R., O'Neil, J.R., Rea, D.K., and Owen, R.M., 1995. Dissociation of oceanic methane hydrate as a cause of the carbon isotope excursion at the end of the Paleocene. Paleoceanography, 10: 965-971.

Dickens, G.R., Castillo, M.M., and Walker, J.C.G., 1997. A blast of gas in the latest Paleocene: Simulating first-order effects of massive dissociation of oceanic methane hydrate. Geology, 25: 259-263.

Dickens, G.R., 2003. Rethinking the global carbon cycle with a large, dynamic and microbially mediated gas hydrate capacitor. Earth and Planetary Science Letters, 213: 169-183.

Driscoll, N.W., Weissel, J.K., and Goff, J.A., 2000. Potential for large-scale submarine slope failure and tsunami generation along the U.S. mid-Atlantic coast. Geology, 28: 407-410.

Egeberg, P.K., and Dickens, G.R., 1999. Thermodynamic and pore water halogen constraints on gas hydrate distribution at ODP Site 997 (Blake Ridge). Chemical Geology, 153: 53-79.

Egorov, A.V., Crane, K., Vogt, P.R., and Rozhkov, A.N., 1999. Gas hydrates that outcrop on the sea floor: stability models. Geo-Marine Letters, 19: 89-96.

Elvert, M., Greinert, J., and Suess, E., 2001. Carbon isotopes of biomarkers derived from methane-oxidizing microbes at Hydrate Ridge, Cascadia Convergent Margin, *in* Paull, C., ed., Natural gas hydrates: Occurrence, distribution, and detection: Geophysical Monograph 124, American Geophysical Union, pp. 115-129.

Flemings, P., Liu, C.-S., and Winters, W.J., 2003. Critical pressure and multiphase flow in Blake Ridge gas hydrates. Geology, 31: 1057-1060.

Formolo, M.J., Lyons, T.W., Zhang, C., Kelley, C.A., Sassen, R., Horita, J., and Cole, D.R., 2004. Quantifying carbon sources in the formation of authigenic carbonates at gas hydrate sites in the Gulf of Mexico. Chemical Geology, 205: 253-264.

Foucher, J.-P., Nouzé, H., Henry, P., 2002. Observation and tentative interpretation of a double BSR on the Nankai slope. Marine Geology 187 (1-2): 161-175.

Froelich, P.N., Kvenvolden, K.A., Torres, M.E., Waseda, A., Didyk, B.M., and Lorenson, T.D., 1995. Geochemical evidence for gas hydrate in sediment near the Chile Triple Junction. *In* Lewis, S.D., Behrmann, J.H., Musgrave, R.J., and Cande, S.C. (Eds.), Proc. ODP, Sci. Results, 141: College Station, TX (Ocean Drilling Program), pp. 279–286.

Gieskes, J.M., Blanc, G., Vrolijk, P., Elderfield, H., and Barnes, R., 1990. Interstitial water chemistry—major constituents. *In* Moore, J.C., Mascle, A., et al., Proc. ODP, Sci. Results, 110: College Station, TX (Ocean Drilling Program), pp. 155–178.

Ginsburg, G.D., Guseynov, R.A., Dadashev, A.A., Telepnev, E.V., Askeri-Nasirov, P.Y., Yesikov, A.A., Mal'tseva, V.I., Mashiroav, Y.G., and Shabayeva, I.Y., 1992. Gas hydrates of the southern Caspian: International Geology Review, 43: 765-782.

Ginsburg, G.D., Soloviev, V.A., Cranston, R.E., Lorenson, T.D., and Kvenvolden, K.A., 1993. Gas hydrates from the continental slope, offshore Sakhalin Island, Okhotsk Sea. Geo-Marine Letters, 13: 41-48.

Ginsburg, G., Milkov, A.V., Soloviev, V.A., Egorov, A.V., Cherkashev, G.A., Vogt, P.R., Crane, K., Lorenson, T.D., and Khutorskoy, M.D., 1999. Gas hydrate accumulation at the Håkon Mosby Mud Volcano. Geo-Marine Letters, 19: 57-67.

Greinert, J., Bohrmann, G., and Suess, E., 2001. Gas hydrate-associated carbonates and methane-venting at Hydrate Ridge: Classification, distribution, and origin of authigenic lithologies, *in* Paull, C. and Dillon W.P. ed., Natural gas hydrates: Occurrence, distribution, and detection: Geophysical Monograph 124: 87-98, American Geophysical Union, pp. 99-113.

Gutt, C., Asmussen, B., Press, W., Merkl, C., Casalta, H., Greinert, J., Bohrmann, G., Tse, J., and Hüller, A., 1999. Quantum rotations in natural methane-clathrates from the Pacific sea-floor. Europhysics Letters, 48: 269-275.

Haeckel, M., Suess, E., Wallmann, K., and Rickert, D., 2004. Rising methane gas bubbles form massive hydrate layers at the seafloor: Geochimica et Cosmochimica Acta, 68: 4335-4345.

Hammerschmidt, E.G., 1934. Formation of gas hydrates in natural gas transmission lines. Industrial and Engineering Chemistry, 26: 851 pp.

Handa, Y.P 1990. Effect of hydrostatic pressure and salinity on the stability of gas hydrates. J Phys. Chem., 94: 2651-2657.

Haq, B.U., 1998. Natural gas hydrates: searching for the long-term climatic and slope-stability records, *in* Henriet, J.P., and Mienert, J., eds., Gas Hydrates: Relevance to World Margin Stability and Climate Change, Volume 137: Special Publications: London, Geological Society, pp. 303-318.

Harrison, W.E., and Curiale, J.A., 1982. Gas hydrates in sediments of holes 497 and 498A, Deep Sea Drilling Project Leg 67, *in* Aubouin, J., and von Huene, R., eds., Initial Reports of the Deep Sea Drilling Project, Volume 67, U.S.Governmental Printing Office, pp. 591-594.

Heeschen, K., Tréhu, A., Collier, R.W., Suess, E., and Rehder, G., 2003. Distribution and height of methane bubble plumes on the Cascadia Margin characterized by acoustic imaging: Geophysical Research Letters, 30: 10.1029/2003GL016974.

Hensen, C., and Wallmann, K., 2005, Methane formation at Costa Rica continental margin - constraints for gas hydrate inventories and cross-décollement fluid flow. Earth and Planetary Science Letters: 236: 41-60.

Hesse, R., and Harrison, W.E., 1981. Gas hydrates (clathrates) causing pore-water freshening and oxygen istope fractionation in deep-water sedimentary

sections of terrigenous continental margins: Earth and Planetary Science Letters, 55: 453-462.

Hesse, R., Lebel, J., and Gieskes, J.M., 1985. Intersitial water chemistry of gas-hydrate bearing sections on the Middle America trench slope, DSDP Leg 84, *in* von Huene, R., and Aubouin, J., eds., Inital Reports of DSDP, Volume 84: Washington, U.S. Governmental Printing Office, p. 727-737.

Hesse, R., 2003. Pore water anomalies of submarine gas-hydrate zones as tool to assess hydrate abundance and distribution in the subsurface - what have we learned in the past decade. Earth-Science Reviews, 61: 149-179.

Hyndman, R.D., and Spence, G.D., 1992. A seismic study of methane hydrate marine bottom-simulating reflectors. Journal Geophys. Res, (97): 6683-6698.

Iversen, N., Jørgensen, B.B. 1985. Anaerobic methane oxidation rates at the sulfate-methane transition in marine sediments from Kattegat and Skagerrak (Denmark). Limnology & Oceanography 30 (5): 944-955.

Joye, S.B., Boetius, A., Orcutt, B.N., Montoya, J.P., Schulz, H.N., Erickson, M.J., and Lugo, S.K. 2004. The anaerobic oxidation of methane and sulfate reduction in sediments from Gulf of Mexico cold seeps. Chemical Geology 205: 219-238

Kastner, M., Elderfield, H., and Martin, J.B., 1991. Fluids in convergent margins: what do we know about their composition, origin, role in diagenesis and importance for oceanic chemical fluxes: Phil. Trans. R. Soc. London A, 335: 243-259.

Kastner, M., Kvenvolden, K.A., and Lorenson, T.D., 1998. Chemistry, isotopic composition, and origin of a methane-hydrogen sulfide hydrate at the Cascadia subduction zone. Earth and Planetary Science Letters, 156: 173-183.

Kennett, J., Cannariato, K., Hendy, I., and Behl, R., 2002. Methane hydrates in Quaternary climate change: the clathrate gun hypothesis, AGU books board, 216 p.

Kuhs, W.F., Bauer, F.C., Hausmann, R., Ahsbahs, H., Dorwarth, R., and Hölzer, K., 1996. Single crystal diffraction with X-rays and neutrons. High quality at high pressure? High Press. Res., 14: 341-352.

Kuhs, W.F., Genov, G.Y., Goreshnik, E., Zeller, A., Techmer, K., and Bohrmann, G. 2004. The impact of porous microstructures of gas hydrates on their macroscopic properties. International Journal of Offshore and Polar Engineering, 14: 305-309.

Kulm, L.D., Suess, E., Moore, J.C., Carson, B., Lewis, B.T., Ritger, S.D., Kadko, D.C., Thornburg, T.M., Embley, R.W., Rugh, W.D., Massoth, G.J., Langseth, M.G., Cochrane, G.R., and Scamann, R.L. 1986, Oregon subduction zone: venting, fauna, and carbonates. Science, 231: 561-566.

Kvenvolden, K.A., and McMenamin, M.A., 1980. Hydrates of natural gas: A review of their geological occurrence. US Geological Survey Circular, 825, 0-11.

Kvenvolden, K.A., 1988, Methane hydrate - a major reservoir of carbon in the shallow geosphere? Chemical Geology, 71: 41-51.

Kvenvolden, K.A., 1998. A primer on the geological occurence of gas hydrate, *in* Henriet, J.P., and Mienert, J., eds., Gas Hydrates: Relevance to World Margin Stability and Climate Change, Volume 137: Special Publications: London, Geological Society, pp. 9-30.

Kvenvolden, K.A., and Kastner, M., 1990. Gas hydrates of the Peruvian outer continental margin, *in* Suess, E., and von Huene, R., (eds.), Proc. ODP., Scien. Results, Volume 112: College Station, pp. 517-526.

Kvenvolden, K.A., 1993. A primer on gas hydrates. In: Howell. D.G. et al. (eds.) The future of energy gases, U.S. geological survey professional paper, 1570: pp. 279-291.

Lein, A., Vogt, P., Crane, K., Egorov, A., and Ivanov, M., 1999. Chemical and isotopic evidence for the nature of the fluid in CH_4-containing sediments of the Håkon Mosby Mud Volcano. Geo-Marine Letters, 19: 76-83.

Maekawa, T., 2004. Experimental study on isotopic fractionation in water during gas hydrate formation: Geochemical Journal, 38:129-138.

Makogon, Y.F., Trebin, F.A., Trofimuk, A.A., Tsarev, V.P., and Cherskiy, N.V. 1971. Detection of a pool of natural gas in a solid (hydrated gas) state: Doklady p. 59-66. Akademii Nauk SSSR.

Mathews, M.A., and von Huene, R., 1985. Site 570 methane hydrate zone, *in* Orlofsky, S., ed., DSDP Initerum Reports, Volume 84, U.S. Gov. Printing Office, pp. 773-790.

Matsumoto, R., and Borowski, W., 2000. Gas hydrate estimates from newly determined oxygen isotopic fractionation and $\delta^{18}O$ anomalies of interstitial waters: Leg 164, Blake Ridge, *in* Paull, C., Matsumoto, R., Wallace, P.J., and Dillon, W.P., (eds.), Proc. ODP, Sci. Results, Volume 164: College Station, TX (Ocean Drilling Program), 196: pp. 203-206.

Mazurenko, L.L., and Soloviev, V.A., 2003. Worldwide distribution of deep-water fluid venting and potential occurrences of gas hydrate accumulations. Geo-Marine Letters, 23: 162-176.

Mienert, J., Posewang, J., and Baumann, M., 1998. Gas hydrates along the northeastern Atlantic margin: possible hydrate-bound margin instabilities and possible release of methane, *in* Henriet, J.-P., and Mienert, J., eds., Gas Hydrates: Relevance to World Margin Stability and Climate Change, Volume 137: London, Geological Society, pp. 275-291.

Nimblett J. ; Ruppel C., 2003. Permeability evolution during the formation of gas hydrates in marine sediments. Journal of Geophysical Research, 108 (B9) pp. EPM 2-1, Cite ID 2420, DOI 10.1029/2001JB001650.

Nisbet, E.G., and Piper, D.J.W., 1998. Giant submarine landslides. Nature, 392: 329-330.

Orphan, V.J., Ussler III, W., Naehr, T.H., House, C.H., Hinrichs, K.-U., and Paull, C.K. 2004. Geological, geochemical, and microbiological heterogeneity of the seafloor around methane vents in the Eel River Basin, offshore California. Chemical Geology 205: 265-289.

Paull, C.K., Ussler III, W., and Dillon, W.P., 1991. Is the

extent of glaciation limited by marine gas-hydrates: Geophysical Research Letters, 18: 432-434.

Paull, C.K., Ussler III, W., and Borowski, W., 1994. Sources of biogenic methane to form marine gas hydrates - In situ production or upward migration?: Annals of the New York Academy of Sciences, 715: 392-409.

Paull, C.K., Matsumoto, R., and Wallace, P.J., 1996. Proceedings of the ODP, Initial Reports: College Station, TX, 623 pp.

Paull, C.K., Matsumoto, R., Wallace, P.J., and Dillon, W.P., 2000, Proceedings of the Ocean Drilling Program, Scientifc Results: College Station TX, 459 pp.

Reed, D.W., Fujita, Y., Delwiche, M.E., Blackwelder, D.B., Sheridan, P.P., Uchida, T., and Colwell, F.S. 2002. Microbial communities from methane-hydrate bearing deep marine sediments in a forearc basin. Applied Environmental Microbiology, 20002, 3759-3770.

Ritger, S., Carson, B., and Suess, E., 1987. Methane-derived authigenic carbonates formed by subduction-induced pore-water expulsion along the Oregon/ Washington margin: Geological Society of America Bulletin, 98: 147-156.

Ruppel, C., Dickens, G.R., Castellini, D.G., Gilhooly, W., and Lizarralde, D., 2005. Heat and salt inhibition of gas hydrate formation in the northern Gulf of Mexico: Geophysical Research Letters**,** 32: L04605, doi:10.1029/2004GL021909.

Sahling, H., Rickert, D., Lee, R.W., Linke, P., and Suess, E., 2002. Macrofaunal community structure and sulfide flux at gas hydrate deposits from the Cascadia convergent margin: Marine Ecology Progress Series, 231: 121-138.

Sample, J., and Reid, M.R., 1998, Contrasting hydrogeological regimes along strike-slip and thrust faults in the Oregon convergent margin: Evidence from the chemistry of syntectonic carbonate cements and veins: GSA Bulletin, 110: 48-59.

Sassen, R., Mac Donald, I.R., Requejo, A.G., Guinasso Jr, N.L., Kennicutt II, M.C., Sweet, S.T., and Brooks, J.M., 1994. Organic geochemistry of sediments from chemosynthetic communities, Gulf of Mexico slope: Geo-Marine Letters, 14: 110-119.

Schoell, M., 1988. Multiple origins of methane in the Earth. Chemical Geology 71 (1-3): 1-10.

Shipley, T.H., Houston, M.H., Buffler, R.T., Shaub, F.J., McMillen, K.J., Ladd, J.W., and Worzel, J.L., 1979. Seismic evidence for widespread possible gas hydrate horizons on continetal slopes and rises. Am. Assoc. Petrol. Geol. Bull., 63: 2204-2213.

Shipley, T.H., and Didyk, B.M., 1982. Occurrence of methane hydrates offshore southern Mexico, *in* Watkins, J.S., and Moore, J.C., eds., Initial Reports of the Deep Sea Drilling Project, Volume 66, U.S. Government Printing Office, pp. 547-555.

Shoji, H., and Langway, C.C., 1982. Air hydrate inclusions in fresh ice core. Nature, 298:548-550.

Sloan, E.D.j., 1998. Physical/chemical properties of gas hydrates and application to world margin stability and climatic change, *in* Henriet, J.P., and Mienert, J., (eds.), Gas Hydrates: Relevance to World Margin Stability and Climate Change, Volume 137: Special Publications: London, Geological Society, pp. 31-50.

Stoll, R.D., Ewing, J.I., and Bryan, G.M., 1971. Anomalous wave velocities in sediments containing gas hydrates: Journal Geophys. Res, 76: 2090-2094.

Suess, E., and Whiticar, M.J., 1989. Methane-derived CO_2 in pore fluids expelled from the Oregon subduction zone. Palaeogeography, Palaeoclimatology, Palaeoecology, 71: 119-136.

Suess, E., Torres, M.E., Bohrmann, G., Collier, R.W., Greinert, J., Linke, L., Rehder, G., Tréhu, A., Wallmann, K., Winckler, G., and Zuleger, E., 1999. Gas hydrate destabilization: enhanced dewatering, benthic material turnover and large methane plumes at the Cascadia convergent margin: Earth and Planetary Science Letters, 170: 1-15.

Suess, E., Torres, M.E., Bohrmann, G., Collier, R.W., Rickert, D., Goldfinger, C., Linke, P., Heuser, A., Sahling, H., Heeschen, K., Jung, C., Nakamura, K., Greinert, J., Pfannkuche, O., Tréhu, A., Klinkhammer, G., Whiticar, M.C., Eisenhauer, A., Teichert, B., and Elvert, E., 2001. Sea floor methane hydrates at Hydrate Ridge, Cascadia Margin, *in* Paull, C. and Dillon W.P. ed., Natural gas hydrates: Occurrence, distribution, and detection: Geophysical Monograph 124: 87-98, American Geophysical Union.

Takahashi, H., Japan Petroleum Exploration Co., L., Yonezawa, T., Corporation, J.N.O., Takedomi, Y., and Ministry of Economy, T.A.I., 2001. Exploration for Natural Gas Hydrate in Nankai-Trough Wells Offshore Japan, Offshore Technology Conference, Volume 13040: Houston, Texas, OTC.

Teichert, B.M.A., Gussone, N., Eisenhauer, A., and Bohrmann, G., 2004. Clathrites - Archives of near-seafloor pore water evolutions (^{44}Ca, ^{13}C, ^{18}O) in seep environments. Geology, 33: 213-216.

Teichert, B.M.A., Bohrmann, G., and Suess, E., 2005a. Chemoherms on Hydrate Ridge: Unique microbially mediated carbonate build ups in cold seep settings. Palaeogeography, Palaeoclimatology, Palaeoecology, 227: 67-85.

Teichert, B.M.A., Bohrmann, G., Torres, M., and Eisenhauer, A., 2005b. Fluid sources, fluid pathways and diagenetic reactions across an accretionary prism revealed by Sr and B geochemistry. Earth and Planetary Science Letters, 239: 106-121.

Tissot, B., and Welte, H., 1992. Petroleum formation and occurrence. Springer-Verlag, 536 pp.

Tomaru, H., Matsumoto, R., Torres, M.E., and Borowski, W.S., subm., Geological and geochemical constraints on the isotopic composition of interstitial waters from the Hydrate Ridge region, Cascadia continental margin.

Torres, M.E., Wallmann, K., Tréhu, A.M., Bohrmann, G., Borowski, W.S., and Tomaru, H., 2004. Gas hydrate growth, methane transport, and chloride enrichment at the southern summit of Hydrate Ridge, Cascadia margin off Oregon. Earth and Planetary Science Letters, 226: 225-241.

Tréhu, A.M, Bohrmann, G., Rack, F.R., Torres, M.E., et al., 2003. Proc. ODP, Init. Repts., 204 [CD-ROM].

Available from: Ocean Drilling Program, Texas A&M University, College Station TX 77845-9547, USA.

Tréhu, A.M., Long, P.E., Torres, M.E., Bohrmann, G., R., R.F., Collett, T.S., Goldberg, D.S., Milkov, A.V., Riedel, M., Schultheiss, P., Bangs, N.L., Barr, S.R., Borowski, W.S., Claypool, G.E., Delwiche, M.E., Dickens, G.R., Gracia, E., Guerin, G., Holland, M., Johnson, J.E., Lee, Y.-J., Liu, C.-S., Su, X., Teichert, B., Tomaru, H., Vanneste, M., Watanabe, M., and Weinberger, J.L., 2004a. Three-dimensional distribution of gas hydrate beneath southern Hydrate Ridge: constraints from ODP Leg 204. Earth and Planetary Science Letters, 222: 845-862.

Tréhu, A.M., Flemings, P.B., Bangs, N.L., Chevallier, J., Gràcia, E., Johnson, J.E., Liu, C.-S., Liu, X., Riedel, M., and Torres, M.E., 2004b. Feeding methane vents and gas hydrate deposits at south Hydrate Ridge. Geophys. Res. Lett., 31:10.1029/2004GL021286.

Tucholke, B.E., Bryan, G.M., and Ewing, J.I., 1977. Gas-hydrate horizons detected in seismic-profiler data from the western North Atlantic. American Association of Petroleum Geologists Bulletin, 61: 698-707.

Ussler III, W., and Paull, C., 2001. Ion exclusion associated with marine gas hydrate deposits, *in* Paull, C., and Dillon, W.P., (eds.), Natural gas hydrates-occurrence, distribution, and detection, Geophysical Monograph 124: Washington, AGU, pp. 41-51.

Weinberger, J.L., Brown, K.M., and Long, P.E., 2005. Painting a picture of gas hydrate distribution with thermal images. Geophysical Research Letters, 32: doi: 10.1029/2004GL021437.

Westbrook, G.K., Carson, B., Musgrave, R.J., et al. 1994. Proceedings, initial reports, Ocean Drilling Program, Leg 146: Cascadia Margin, 611 pp.

Whiticar, M.J., 1999. Carbon and hydrogen isotope systematics of bacterial formation and oxidation of methane. Chemical Geology, 161: 291-314.

Whiticar, M.J., Faber, E., and Schoell, M., 1986. Biogenic methane formation in marine and freshwater environments. CO_2 reduction vs. Acetate fermentation - Isotope evidence. Geochimica et Cosmochimica Acta, 50: 693-709.

Vasil'ev, V.G., Makogon, Y.F., Trebin, F.A., A.A., T., and Cherskiy, N.V., 1970. The property of natural gases to occur in the Earth crust in a solid state and to form gas hydrate deposits. Otkrytiya v SSR, pp. 15-17.

von Stackelberg, M., and Müller, H.R., 1954. Feste Gashydrate II: Struktur und Raumchemie. Z. Elektrochem., 58: 25-39.

Wellsbury, P., Goodman, K., Cragg, B.A., and Parkes, R.J., 2000. The geomicrobiology of deep marine sediments from Blake Ridge containing methane hydrate (Sites 994, 995 and 997), *in* Paull, C., Matsumoto, R., Wallace, P.J., and Dillon, W.P., eds., Proceeding of ODP, Volume 164: 379-391.

Wood, B.J., and Ruppel, C., 2000. Seismic and thermal investigations of the Blake Ridge gas hydrate area: a synthesis, *in* Paull, C., Matsumoto, R., Wallace, P.J., and Dillon, W.P., (eds.), Proceedings of ODP, Scientific Results, Volume 164: 253-264.

Xu, W., and Ruppel, C., 1999. Predicting the occurrence, distribution, and evolution of methane gas hydrate in porous marine sediments. Journal of Geophysical Research, 104: 5081-5095.

Yakushev, V.S., and Istomin, V.A., 1992. Gas-hydrate self-preservation effect, *in* Maeno, N., and Hondoh, T., (eds.) Sapporo, Hokkaido University Press, pp. 136-140.

Yefremova, A.G., and Zhizchenko, B.P., 1974. Occurrence of crystal hydrates of gases in the sediments of modern marine basins. Doklady Akademii Nauk SSSR, 214: 1,179-1,181.

Zatsepina, O.Y., and Buffett, B.A., 1997. Phase equilibrium of gas hydrate: implications for the formation of hydrate in the deep sea-floor. Geophysical Research Letters, 24: 1567-1570.